NASA TECHNICAL MEMORANDUM

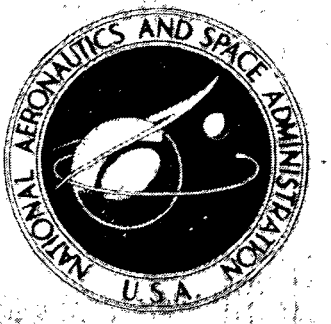

NASA TM X-2790

NASA TM X-2790

ANALYSIS OF THE DYNAMICS OF THIN PRIMARY MIRRORS FOR LARGE ASTRONOMICAL TELESCOPES

by Aaron J. Ostroff and Mary McCann

Langley Research Center
Hampton, Va. 23665

NATIONAL AERONAUTICS AND SPACE ADMINISTRATION • WASHINGTON, D. C. • JULY 1973

1. Report No.	2. Government Accession No.	3. Recipient's Catalog No.
NASA TM X-2790		

4. Title and Subtitle	5. Report Date
ANALYSIS OF THE DYNAMICS OF THIN PRIMARY MIRRORS FOR LARGE ASTRONOMICAL TELESCOPES	July 1973
	6. Performing Organization Code

7. Author(s)	8. Performing Organization Report No.
Aaron J. Ostroff (Langley Research Center) and Mary McCann (Vought Missiles and Space Company)	L-8893
	10. Work Unit No. 188-78-57-05
9. Performing Organization Name and Address	11. Contract or Grant No.
NASA Langley Research Center Hampton, Va. 23665	
	13. Type of Report and Period Covered
12. Sponsoring Agency Name and Address	Technical Memorandum
National Aeronautics and Space Administration Washington, D.C. 20546	14. Sponsoring Agency Code

15. Supplementary Notes

16. Abstract

The NASTRAN structural analysis program has been used to investigate the dynamic properties of thin primary mirrors suitable for use in large orbiting astronomical telescopes. One application for which the dynamic properties of large flexible mirrors are necessary is figure error control of the primary mirror. This paper includes an analysis of the mode shapes and modal frequencies for several thin, homogeneous, isotropic mirrors. Typical cases include two different mirror diameters, two different diameter-to-thickness ratios, and both a mirror without and a mirror with a central hole that is 22 percent of the mirror diameter.

The finite-element structural model is first evaluated by comparing the NASTRAN generated results with theoretical values for a simply supported, flat, circular mirror. The same model is then used for the spherical mirrors evaluated in the remainder of this paper. The results for a spherical mirror will be very similar to those for a parabolic mirror because the distance between surfaces is small compared to the thickness of the mirror. The mode shapes and frequencies of a 0.762-meter-diameter mirror with a 60-to-1 diameter-to-thickness ratio and a three-point rigid kinematic (not overconstrained) mount are calculated and plotted for comparison with results obtained previously from the SAMIS structural analysis program for this same mirror. A static analysis is also shown for comparison with experimentally obtained influence coefficients. Masses corresponding to actuator pads are then attached to 58 points on the finite-element model to observe the effect on the natural frequency of vibration. A central hole is incorporated into the mirror and both the diameter and diameter-to-thickness ratio are changed. Inclusion of a hole that is 22 percent of the diameter reveals a slightly more flexible mirror than one with a solid center, with essentially unchanged mode shapes. Contour plots of the first several modes for each configuration are included.

17. Key Words (Suggested by Author(s))	18. Distribution Statement
Astronomical telescope Eigenvectors Eigenvalues NASTRAN Thin mirrors Influence coefficients	Unclassified – Unlimited

19. Security Classif. (of this report)	20. Security Classif. (of this page)	21. No. of Pages	22. Price*
Unclassified	Unclassified	62	$3.00

*For sale by the National Technical Information Service, Springfield, Virginia 22151

ANALYSIS OF THE DYNAMICS OF THIN PRIMARY MIRRORS FOR LARGE ASTRONOMICAL TELESCOPES

By Aaron J. Ostroff and Mary McCann*
Langley Research Center

SUMMARY

The NASTRAN structural analysis program has been used to investigate the dynamic properties of thin primary mirrors suitable for use in large orbiting astronomical telescopes. One application for which the dynamic properties of large flexible mirrors are necessary is figure error control of the primary mirror. This paper includes an analysis of the mode shapes and modal frequencies for several thin, homogeneous, isotropic mirrors. Typical cases include two different mirror diameters, two different diameter-to-thickness ratios, and both a mirror without and a mirror with a central hole that is 22 percent of the mirror diameter.

The finite-element structural model is first evaluated by comparing the NASTRAN generated results with theoretical values for a simply supported, flat, circular mirror. The same model is then used for the spherical mirrors evaluated in the remainder of this paper. The results for a spherical mirror will be very similar to those for a parabolic mirror because the distance between surfaces is small compared to the thickness of the mirror. The mode shapes and frequencies of a 0.762-meter-diameter mirror with a 60-to-1 diameter-to-thickness ratio and a three-point rigid kinematic (not overconstrained) mount are calculated and plotted for comparison with results obtained previously from the SAMIS structural analysis program for this same mirror. A static analysis is also shown for comparison with experimentally obtained influence coefficients. Masses corresponding to actuator pads are then attached to 58 points on the finite-element model to observe the effect on the natural frequency of vibration. A central hole is incorporated into the mirror and both the diameter and diameter-to-thickness ratio are changed. Inclusion of a hole that is 22 percent of the diameter reveals a slightly more flexible mirror than one with a solid center, with essentially unchanged mode shapes. Contour plots of the first several modes for each configuration are included.

---

*Vought Missiles and Space Company.

INTRODUCTION

During the past several years, a great deal of interest has been generated in the area of sensing and controlling the figure error of a primary mirror suitable for large orbiting telescopes. By using figure error control, diffraction-limited tolerances can be maintained despite initial figure errors and external disturbances such as launch stresses, thermal environment, and gravity release.

References 1 and 2 describe an approach that treats the mirror as a flexible structure, the figure of which is regulated by forces acting at discrete points on its rear surface. The ability to maintain diffraction-limited tolerances by this method is a function of the physical properties of the mirror, external disturbances, the control law, and both actuator and figure error sensing locations. By using modal analysis, Creedon and Lindgren (ref. 3) have developed a control law in which the deformation of the physical mirror with its supporting structure is described by an infinite series of the modes of free vibration. Inherent in the design of a modal control system is the requirement for a knowledge of the mode shapes (eigenvectors) and frequencies (eigenvalues) of the mirror. A theoretical technique for designing mirror control systems based on the use of this information has been developed (ref. 4) and experimental tests (ref. 1) have been performed by using a 0.762-meter-diameter, thin, homogeneous, isotropic, spherical mirror with a 60-to-1 diameter-to-thickness ratio. For an astronomical telescope the primary mirror will probably be much larger and will have a central hole. The purpose of this paper is to analyze the mode shapes and modal frequencies for several mirror sizes, both with and without central holes. The structural model is first evaluated by using a flat, circular mirror to compare theoretical results with numerical values. This model, with appropriate out-of-plane coordinates, is then used for the 0.762-meter-diameter spherical mirror to compare with previous results from reference 4. The distance between the surfaces of a spherical and parabolic mirror is very small compared to the thickness of the mirrors analyzed, and the results should be essentially the same for both mirrors. The spherical configuration was maintained to establish continuity throughout this paper. Other configurations include the addition of masses at the rear of the mirror to simulate the mass of actuators and pads and the changing of supporting mount locations. A central hole is then incorporated into the mirror, and finally both the diameter and diameter-to-thickness ratio of the mirror are changed.

SIMPLY SUPPORTED, FLAT, CIRCULAR MIRROR

A test case for which the natural frequencies of vibration are theoretically known consisted of analyzing a flat, circular mirror with a simple circumferential support.

The numerical results obtained from the NASTRAN structural analysis program were compared with theoretical values to determine relative accuracy. The finite-element structural model chosen was identical with that used by Howell and Creedon (ref. 4) so as to minimize differences between their results obtained from the SAMIS structural analysis program and the NASTRAN numerical results for a spherical mirror that is described in the next section. The mirror model is shown in figure 1 and consists of 462 triangular elements and 253 grid points. For best numerical accuracy all elements, except those on the exterior boundary, are equilateral triangles. The numbering system used in this analysis was chosen to minimize the bandwidth of the stiffness and mass matrices for minimum storage and solution times (ref. 5).

Table I contains a list of the material and physical properties for the flat, circular mirror. These properties were also used for the spherical mirrors described subsequently, except where differences are noted.

TABLE I.- MIRROR PROPERTIES

Material	Fused silica
Young's modulus, N/m^2	6.89×10^{10}
Poisson's ratio	0.2
Mass density, kg/m^3	2.2×10^3
Physical properties:	
Outside diameter, m	0.762
Inside diameter, m	0
Diameter-thickness ratio	60
Shape	Flat, circular
Mirror support	Simple

The theoretical eigenvalue solutions for the plate described in table I have been calculated by substituting the appropriate boundary conditions and material properties into the plate equations. (See, for example, ref. 6.) Table II shows a comparison of the NASTRAN numerical results with the theoretical eigenvalues for the first 30 modes. The last column shows that the error in NASTRAN is less than 1 percent for all 30 eigenvalues compared. In general, the NASTRAN data are lower than the theoretical values for the first 12 modes and higher for the remaining modes. Based upon these results, the finite-element structural model shown in figure 1 should be adequate to evaluate a relatively flat, spherical mirror.

TABLE II.- EIGENVALUES FOR SIMPLY SUPPORTED, FLAT, CIRCULAR MIRROR

Mode	Theoretical, $(rad/sec)^2$	NASTRAN, $(rad/sec)^2$	% error in NASTRAN
1	0.477129×10^6	0.476470×10^6	-0.138
2	3.95560	3.95046	-.130
3	3.95560	3.95049	-.118
4	13.5572	13.5231	-.252
5	13.5572	13.5311	-.193
6	18.2812	18.308	.147
7	33.1120	32.9751	-.413
8	33.1120	33.0559	-.169
9	48.7978	48.9003	.210
10	48.7978	48.9125	.235
11	67.1295	66.8906	-.356
12	67.1295	66.9264	-.303
13	102.232	102.495	.257
14	102.232	102.536	.297
15	114.372	114.892	.455
16	120.778	120.257	-.431
17	120.778	120.467	-.257
18	186.047	186.325	.149
19	186.047	186.982	.503
20	199.866	199.143	-.362
21	199.866	199.185	-.341
22	219.867	221.258	.633
23	219.867	221.343	.671
24	308.417	308.856	.142
25	308.417	309.474	.343
26	310.835	309.552	-.413
27	310.835	310.530	-.098
28	375.627	378.382	.733
29	375.627	378.524	.771
30	398.473	402.294	.959

SPHERICAL TEST MIRROR

Modal Analysis

The previously described finite-element structural model with appropriate out-of-plane coordinates was also used to analyze a spherical mirror with a 4.5212-meter radius of curvature and a three-point rigid kinematic mount located at grid points 15, 119, and 247 (fig. 1). Grid point 15 was constrained in all three translational directions; grid point 247 was constrained only in the out-of-plane direction; grid point 119 was constrained in the out-of-plane direction and one inplane direction. All other mirror material and physical properties were identical to those described in table I. The purpose of analyzing this mirror was to compare the NASTRAN numerical data with the SAMIS program results, previously obtained by Howell and Creedon (ref. 4), and with experimental data (ref. 1).

All input and output data were defined with respect to a spherical coordinate system, whereas the constraints for the support points were defined in a rectangular coordinate system (ref. 5). For the remainder of this paper all mode shapes (eigenvectors) are described by the component of displacement normal to the mirror surface.

The Givens method (ref. 5), which uses a tridiagonalization technique, was selected for the normal mode analysis. The number of degrees of freedom for the structural model used was reduced from 1518 to 250 by using a combination of partitioning techniques and the Guyan reduction (ref. 5) within the NASTRAN rigid format. One advantage of the Givens method is that all 250 eigenvalues can be calculated in a single run. In order to compare the SAMIS and NASTRAN results, the SAMIS eigenvalue (ref. 4) must first be related to the NASTRAN eigenvalue by

$$\lambda_N = \frac{1}{\rho_m t \lambda_S}$$

where λ_N is the NASTRAN eigenvalue, λ_S is the SAMIS eigenvalue, ρ_m is the mass density, and t is the mirror thickness. The natural frequency f is related to the NASTRAN eigenvalue by

$$f = \frac{1}{2\pi}\sqrt{\lambda_N}$$

and is plotted in figure 2 for the first 58 modes. Both sets of data, SAMIS and NASTRAN, agree very closely for all modes and establish confidence in the numerical results. The third curve in the figure represents the results obtained by adding masses to 58 different points on the mirror. These masses simulate the mass of Invar pads, which were used

to couple actuator forces into the experimental mirror (ref. 1). For a spherical mirror, the longer pads are located on the circumference and the shortest pad is at the center. Table III shows the location and mass of all 58 pads. With the addition of these pad masses, the total mass of the mirror is increased from 12.679 kg to 14.812 kg; this is a factor of 1.168. Because the natural frequency is inversely proportional to the square root of the increase in mass, the results should be approximately 0.925 times the natural frequencies for the mirror without masses. An analysis of the frequency curves in figure 2 shows this factor to be fairly constant for all modes.

TABLE III.- PAD MASSES AND LOCATION ON MIRROR

Grid point	Mass, kg
127	0.0288
93, 95, 125, 129, 159, 161	.0298
62, 91, 97, 157, 163, 192	.0319
60, 64, 123, 131, 190, 194	.0329
33, 35, 58, 66, 89, 99, 155, 165, 188, 196, 219, 221	.0357
31, 37, 121, 133, 217, 223	.0376
11, 56, 68, 186, 198, 243	.0408
9, 13, 29, 39, 87, 101, 153, 167, 215, 225, 241, 245	.0419
7, 135, 239	.0481

Contour plots for the first 10 mode shapes, normalized to -100, are shown in figure 3. The numbers on these maps indicate the percent of the maximum amplitude and the direction with respect to the peak point of -100. These mode shapes are the same for the two NASTRAN runs described and very similar to the SAMIS results (ref. 4). The three triangles on the contour maps show the locations of the kinematic support points on the boundary.

Static Analysis

A complete set of influence coefficients (elements of the flexibility matrix) were obtained by a simple alteration of the NASTRAN rigid format. (See appendix.) The technique involves the inversion of the stiffness matrix after all constraints have been eliminated.

An analysis of the flexibility matrix indicates that the mirror essentially has six-fold symmetry; the six portions are obtained by drawing diametrical lines from the three

support points (15, 119, 247 in fig. 1). By applying forces to only one-sixth of the mirror, influence coefficients can be obtained for the complete mirror. Table IV shows the calculated displacements normal to the mirror surface for six points on the mirror, owing to a force of 4.448 newtons (1 pound) in the normal direction. The small differences in mirror deflection at these six points are caused by the three-point kinematic mount. If a three-point simple support was used, all displacements would be equal.

TABLE IV.- INFLUENCE COEFFICIENTS AT SIX POINTS

Location of force, grid point	Location of displacement, grid point	Displacement, μm
35	64	1.65114
66	64	1.62917
89	123	1.63094
155	123	1.63993
196	194	1.63814
221	194	1.63686

The numerical results obtained from NASTRAN were compared with the experimental data (ref. 1). Figure 4 shows a comparison of the mirror displacements across one diameter of the mirror (grid points 119 to 135) for the 14 different load locations. The grid point numbers where the loads were applied are 121, 123, 125, 127, 153, 155, 157, 159, 186, 188, 190, 215, 217, and 239. The one case where a significant difference exists between two sets of data is for a force applied to grid point 121. Because grid point 121 is located near a support point (grid point 119), the mirror displacements should be smaller than with the same force applied to grid point 123. The NASTRAN results show smaller peak displacements, whereas the experimental data have the opposite results (figs. 4(a) and 4(b)). For this reason, the experimental data shown in figure 4(a) are believed to be in error.

Interior Kinematic Mount

An analysis was made to investigate the effect of a slight change in mirror-mount location. The three-point kinematic support was moved toward the center of the mirror by 0.0467 meter to grid points 25, 120, and 236. Contour plots for the first seven modes are shown in figure 5 and appear to be very similar to the plots shown in figures 3(a) to 3(g). The main difference is the change in the nodal lines. For example, mode 3 has a nodal line through each support point shown by the crosses in figure 5(c), whereas previously mode 3 did not have a nodal line (fig. 3(c)). This type of shift can significantly

change the desired force pattern on a flexible mirror when used in an active control system (ref. 4). The natural-frequency curve is similar to the NASTRAN results shown in figure 2.

Spherical Mirrors With Central Holes

Large orbiting astronomical telescopes will probably have a Cassegrain-type design, which has a central hole in the primary mirror (refs. 7 and 8). As an example, the primary mirror may have an f-number of approximately 3 and a maximum central hole that is approximately 20 percent of the outside diameter (ref. 8). In order to maintain continuity with the analysis made on the mirrors without holes, a spherical mirror with the same f-number of approximately 2.97 was continued for all cases. The central hole is 22 percent of the mirror diameter and should allow worst case variations from the mirror without any hole. Modal analysis results in this section are for 0.762-meter-diameter (30-inch) and 3.048-meter-diameter (120-inch) mirrors with a 60-to-1 diameter-to-thickness ratio and for a 3.048-meter-diameter mirror with a 20-to-1 ratio. All mirrors have a three-point rigid kinematic mount located at the outer edge of the mirror. Other mirror properties are the same as shown in table I.

Contour plots for the two 60-to-1 diameter-to-thickness-ratio mirrors are identical and are shown in figure 6 for the first seven modes. A comparison of these plots with those for the mirror without any hole (figs. 3(a) to 3(g)) shows that the inclusion of a large central hole has relatively little effect on the mode shapes. The inclusion of a central hole results in a slightly more flexible mirror. The fundamental frequency for the 0.762-meter-diameter mirror decreased by 4.84 percent from 81.0 hertz to 77.1 hertz. Most of the higher modes have a smaller percentage change in frequency. A plot of frequency as a function of mode number for both the 0.762-meter- and 3.048-meter-diameter mirrors with central holes is shown in figure 7. The natural frequencies of the larger mirror are lower by a factor of 4.

The middle curve in figure 7 is for the larger size mirror with a 20-to-1 diameter-to-thickness ratio. The natural frequencies for this mirror are approximately three times greater than those for the thinner mirror with the same diameter. Figure 8 shows the contour plots for the first seven modes of the 20-to-1 ratio case. There are a few slight differences between these plots and those for the thinner mirror (fig. 6). Modes 5, 6, and 7, which have eigenvalues of approximately the same magnitude, have altered positions from the previous case. Mode 7 for the thicker mirror (fig. 8(g)) is very similar to mode 5 for the thinner mirror (fig. 6(e)), and modes 5 and 6 for the thicker mirror (figs. 8(e) and 8(f)) are similar to modes 6 and 7, respectively, for the thinner mirror (figs. 6(f) and 6(g)). Some of the nodal lines of other modes have slightly altered locations on the mirror. In general, the mode shapes of mirrors with central holes as large

as 22 percent of the outside diameter are very similar to the mode shapes for mirrors without holes.

From the analysis of the three mirrors with central holes, the natural frequencies of vibration can be predicted for any mirror within the diameter and thickness ranges of the test cases when the same mounting arrangement, f-number, and material properties are assumed. Figure 9 shows a plot of the fundamental frequency as a linear function of mirror diameter for a mirror with a central hole that is 22 percent of the outside diameter and a 60-to-1 diameter-to-thickness ratio. The two data points show that a diameter increase by a factor of 4 results in a frequency decrease by the same amount. A plot of the fundamental frequency as a function of the diameter-to-thickness ratio for a 3.048-meter-diameter mirror with the same size central hole is shown in figure 10. An increase in the ratio by a factor of 3 results in a frequency decrease by the same amount.

CONCLUDING REMARKS

A dynamic analysis has been made for a large telescope primary mirror to observe the effect of various physical characteristics on the natural modes of vibrations and the natural frequencies. The finite-element structural model was evaluated by analyzing a simply supported, flat, circular mirror which has known eigenvalues. The first 30 eigenvalues calculated by the NASTRAN structural analysis program agree with theoretical values within 1 percent. Based upon these results, the mirror model should be adequate to evaluate a relatively flat, spherical mirror.

The first spherical mirror evaluated had a solid center and is the same mirror previously analyzed by using the SAMIS program. Excellent agreement was found between SAMIS and NASTRAN calculated natural frequencies and mode shapes of the mirror. The addition of 58 scalar masses to grid points on the NASTRAN mirror model to simulate mass pads used in the experimental analysis resulted in a decrease in natural frequency by approximately the predicted amount. A static analysis reveals that the flexibility matrix for this mirror essentially has sixfold symmetry. The small differences in the six areas are caused by the three-point kinematic mount. In general, for the static analysis, good agreement exists between the NASTRAN numerical results and experimental data. An analysis made to investigate the effect of small changes in support-point locations shows relatively little change in modal response. The main change is the shift of node lines through support locations.

A typical large orbiting telescope will have a primary mirror with a central hole. Inclusion of the largest expected hole size reveals a slightly more flexible mirror than one with a solid center, with essentially unchanged mode shapes. Variation of the

diameter and thickness for this mirror shows that the fundamental natural frequency is inversely proportional to the mirror diameter for a constant diameter-to-thickness ratio and is inversely proportional to the diameter-to-thickness ratio for a constant mirror diameter.

Langley Research Center,
National Aeronautics and Space Administration,
Hampton, Va., May 18, 1973.

APPENDIX

TECHNIQUE FOR OBTAINING FLEXIBILITY MATRIX

A complete set of influence coefficients (elements of the flexibility matrix) can be calculated in one NASTRAN run by a simple alteration of the NASTRAN rigid format. The technique involves the inversions of the stiffness matrix KLL to obtain the flexibility matrix FLEX.

The DMAP statements inserted into rigid format 1 of Level 12 are

```
ALTER 90
SOLVE KLL, /FLEX/C,N,1/C,N,1/C,N,2/C,N,2  $
MATGPR GPL, USET,SIL,FLEX //C,N,2/C,N,2  $
ENDALTER
```

Subroutine SOLVE calculates the output matrix FLEX from the equation

$$[KLL][FLEX] = [I]$$

where the identity matrix was obtained by purging the second input to SOLVE.

REFERENCES

1. Robertson, Hugh J.: Evaluation of the Thin Deformable Active Optics Mirror Concept. NASA CR-2073, 1972.

2. Robertson, Hugh J.: Development of an Active Optics Concept Using a Thin Deformable Mirror. NASA CR-1593, 1970.

3. Creedon, J. F.; and Lindgren, A. G.: Control of the Optical Surface of a Thin, Deformable Primary Mirror With Application to an Orbiting Astronomical Observatory. Automatica, vol. 6, no. 5, Sept. 1970, pp. 643-660.

4. Howell, W. E.; and Creedon, J. F.: A Technique for Designing Active Control Systems for Astronomical-Telescope Mirrors. NASA TN D-7090, 1973.

5. MacNeal, Richard H., ed.: The NASTRAN Theoretical Manual. NASA SP-221, 1970.

6. Leissa, Arthur W.: Vibration of Plates. NASA SP-160, 1969.

7. Anon.: Technology Study for a Large Orbiting Telescope. 70-9443-1 (Contract NASw-1925), Opt. Syst. Div., Itek Corp., May 15, 1970. (Available as NASA CR-110253.)

8. Anon.: Large Space Telescope – Continuation of a Technology Study. Itek 71-9463-2 (Contract NASw 2174), Opt. Syst. Div., Itek Corp., Sept. 3, 1971. (Available as NASA CR-122851.)

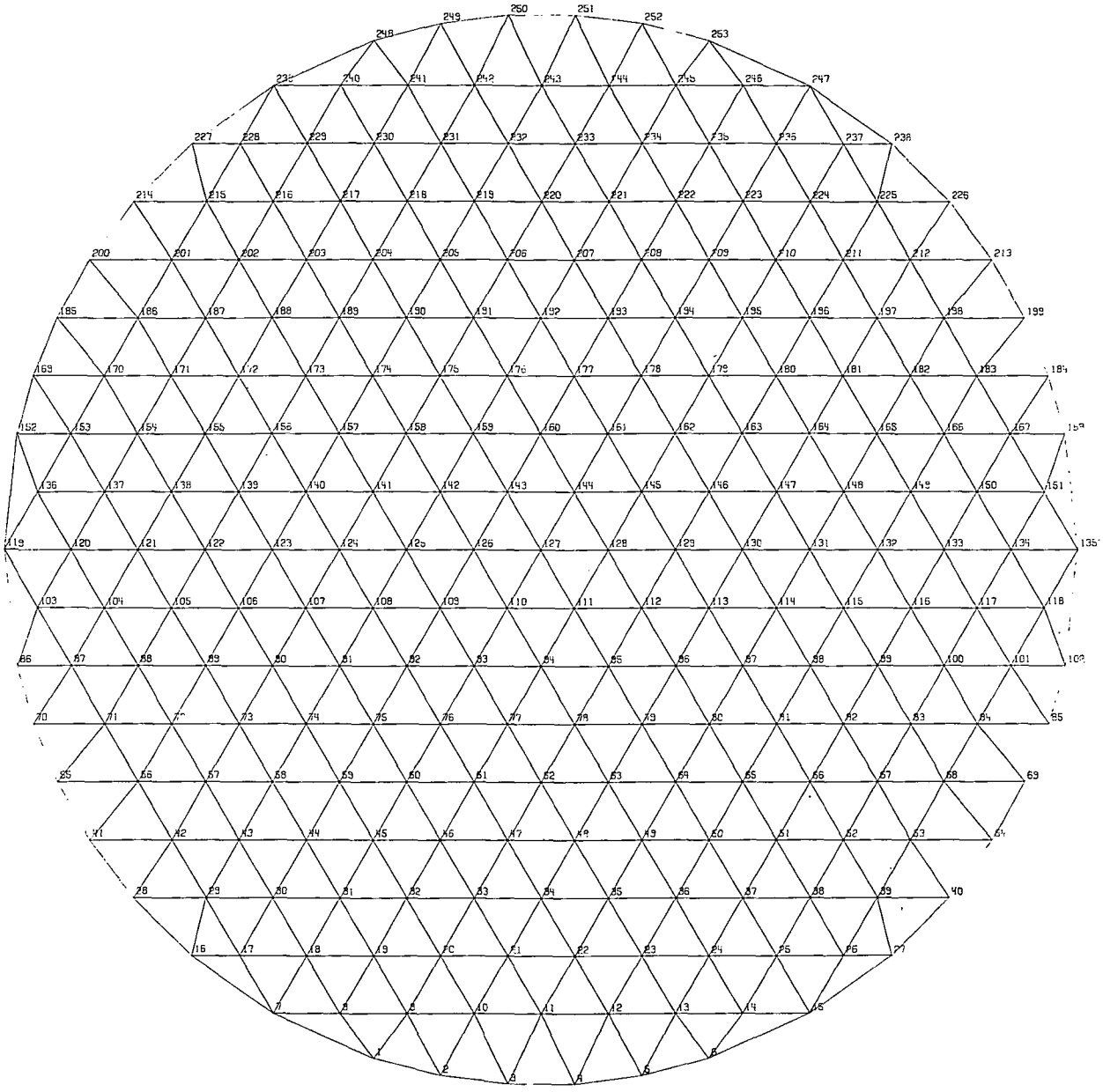

Figure 1.- Finite-element structural model.

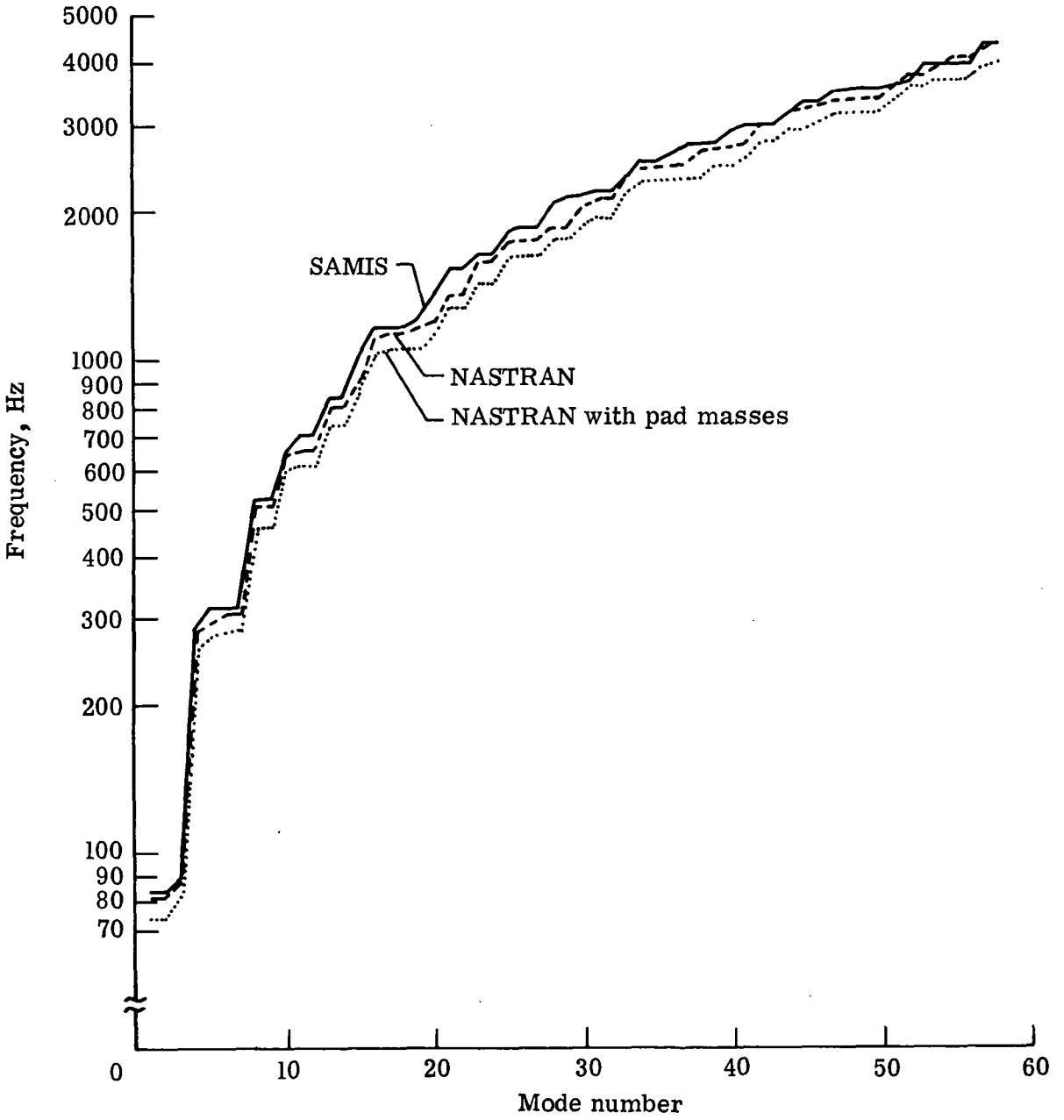

Figure 2.- Modal frequency distribution for 0.762-meter-diameter solid spherical mirror with 60-to-1 diameter-to-thickness ratio for comparison of SAMIS and NASTRAN data.

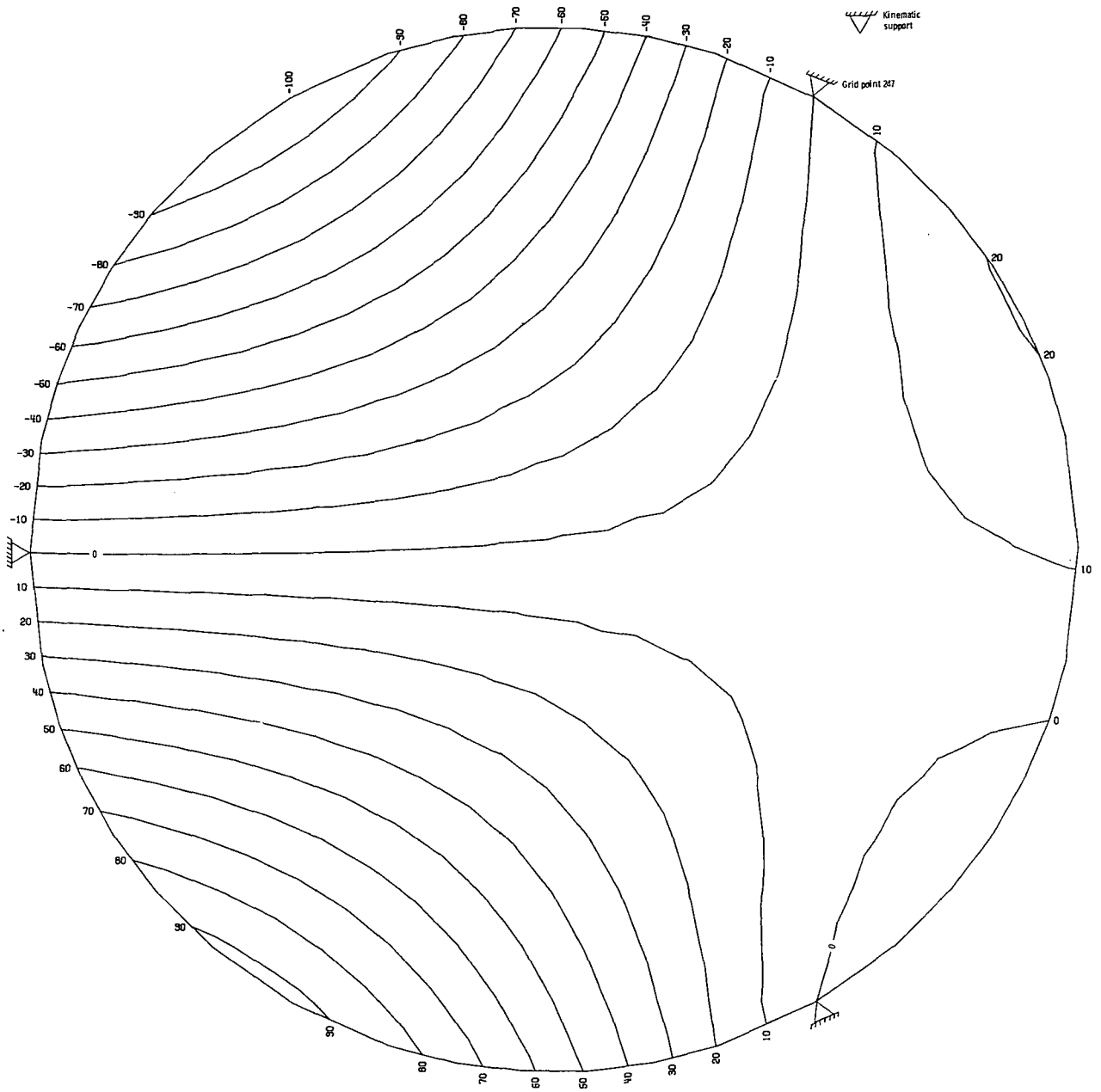

(a) Mode 1.

Figure 3.- Contour plot for 0.762-meter-diameter solid spherical mirror with 60-to-1 diameter-to-thickness ratio and kinematic mount at grid points 15, 119, and 247.

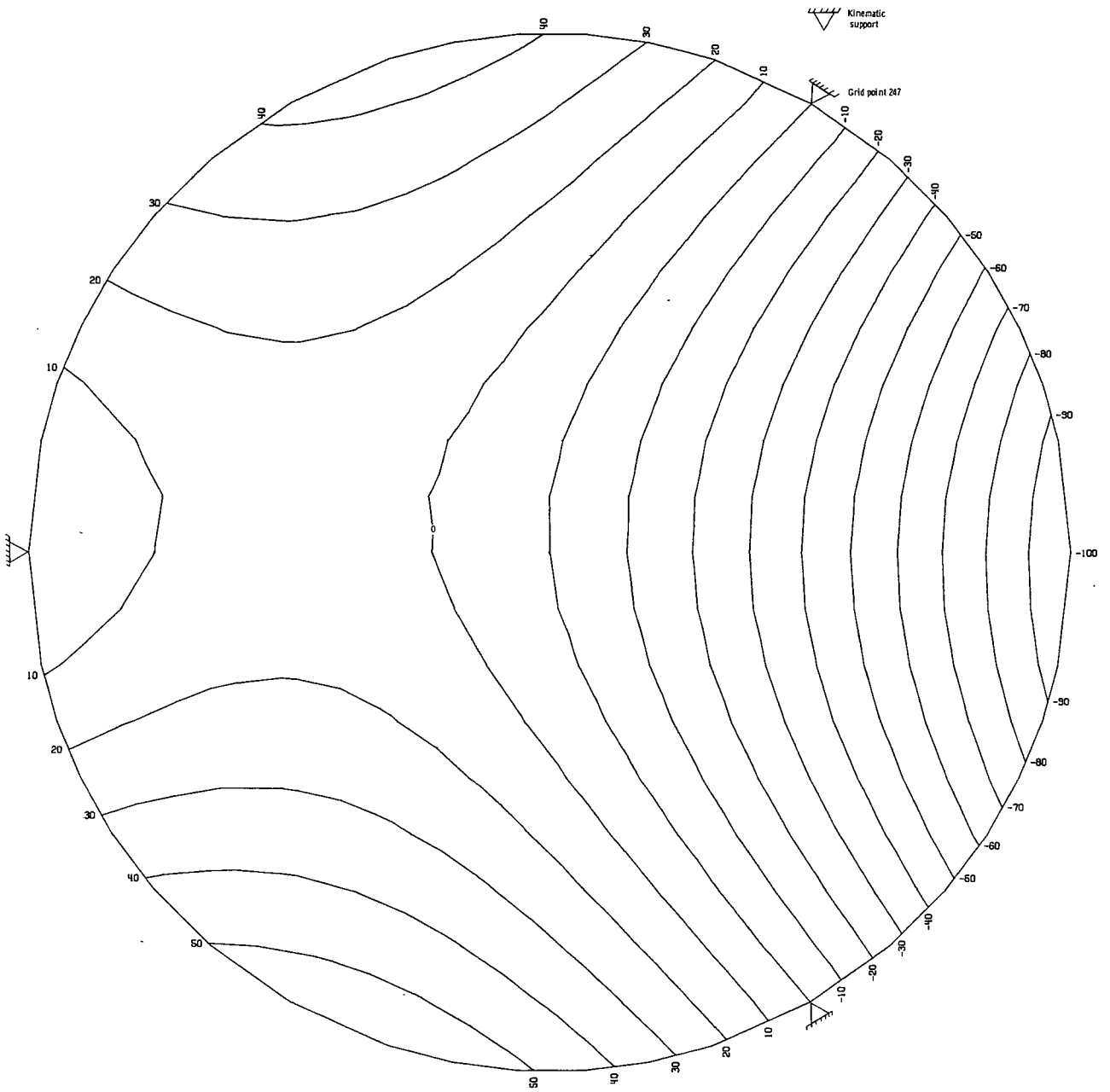

(b) Mode 2.

Figure 3.- Continued.

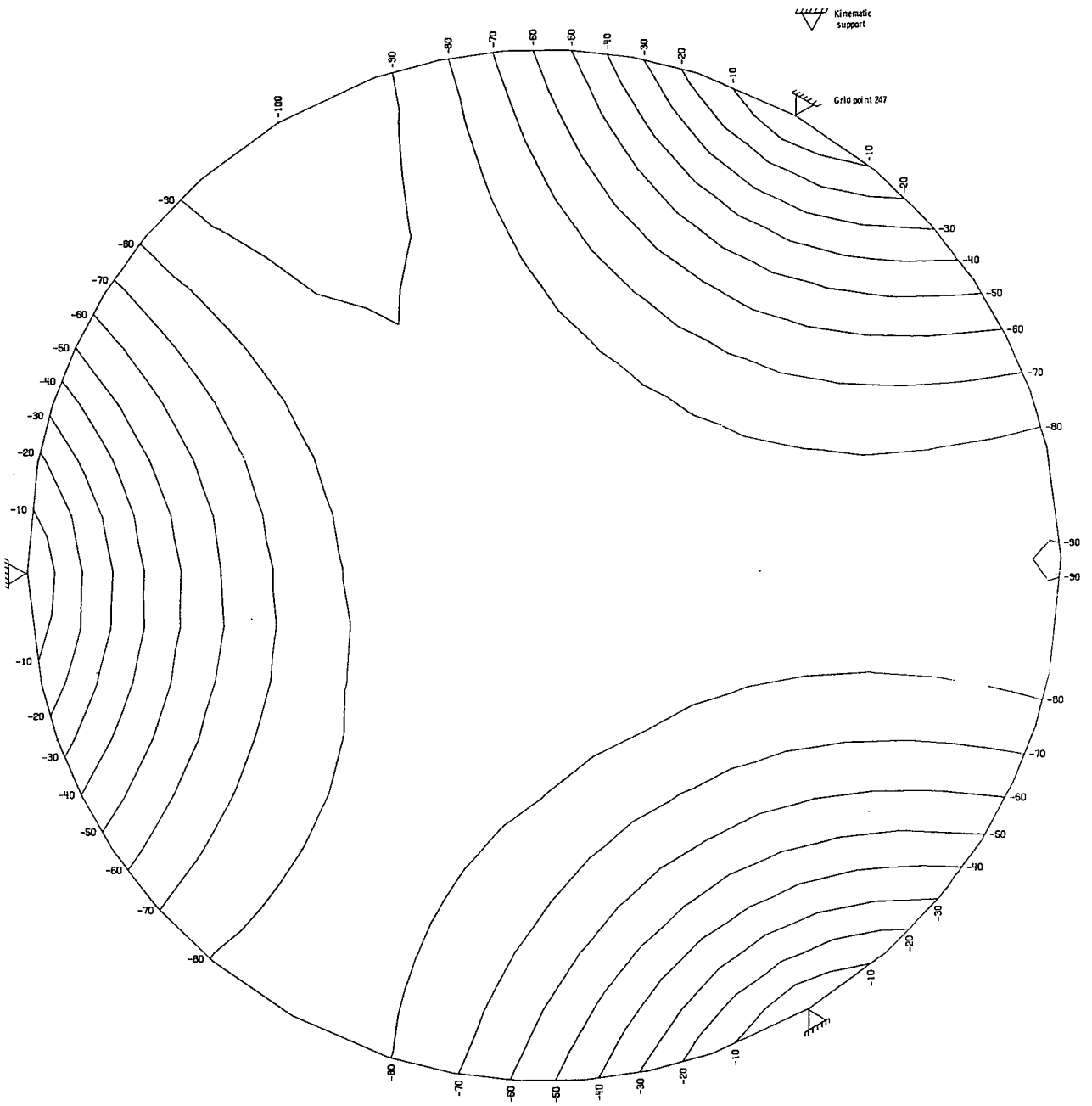

(c) Mode 3.

Figure 3.- Continued.

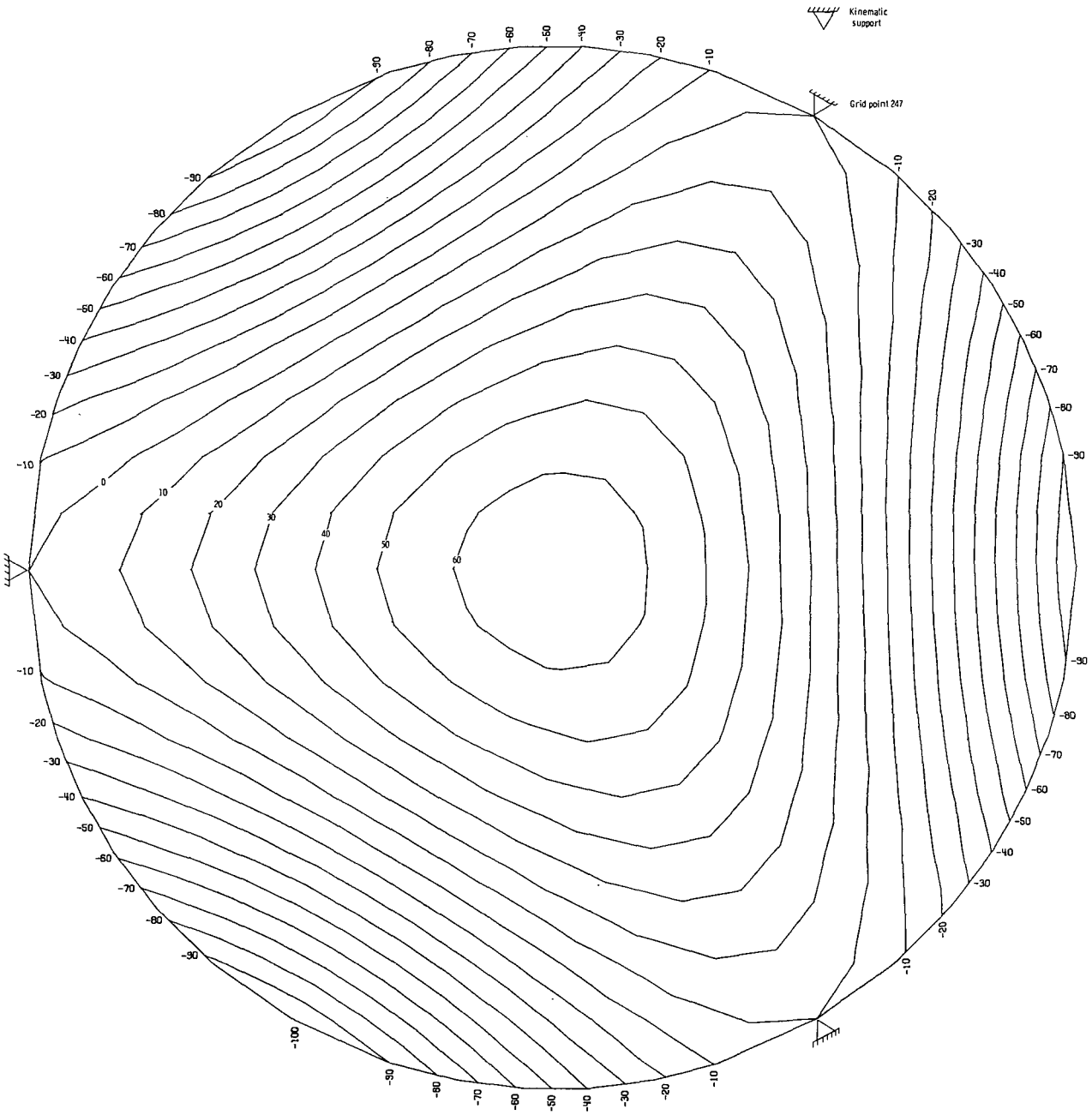

(d) Mode 4.

Figure 3.- Continued.

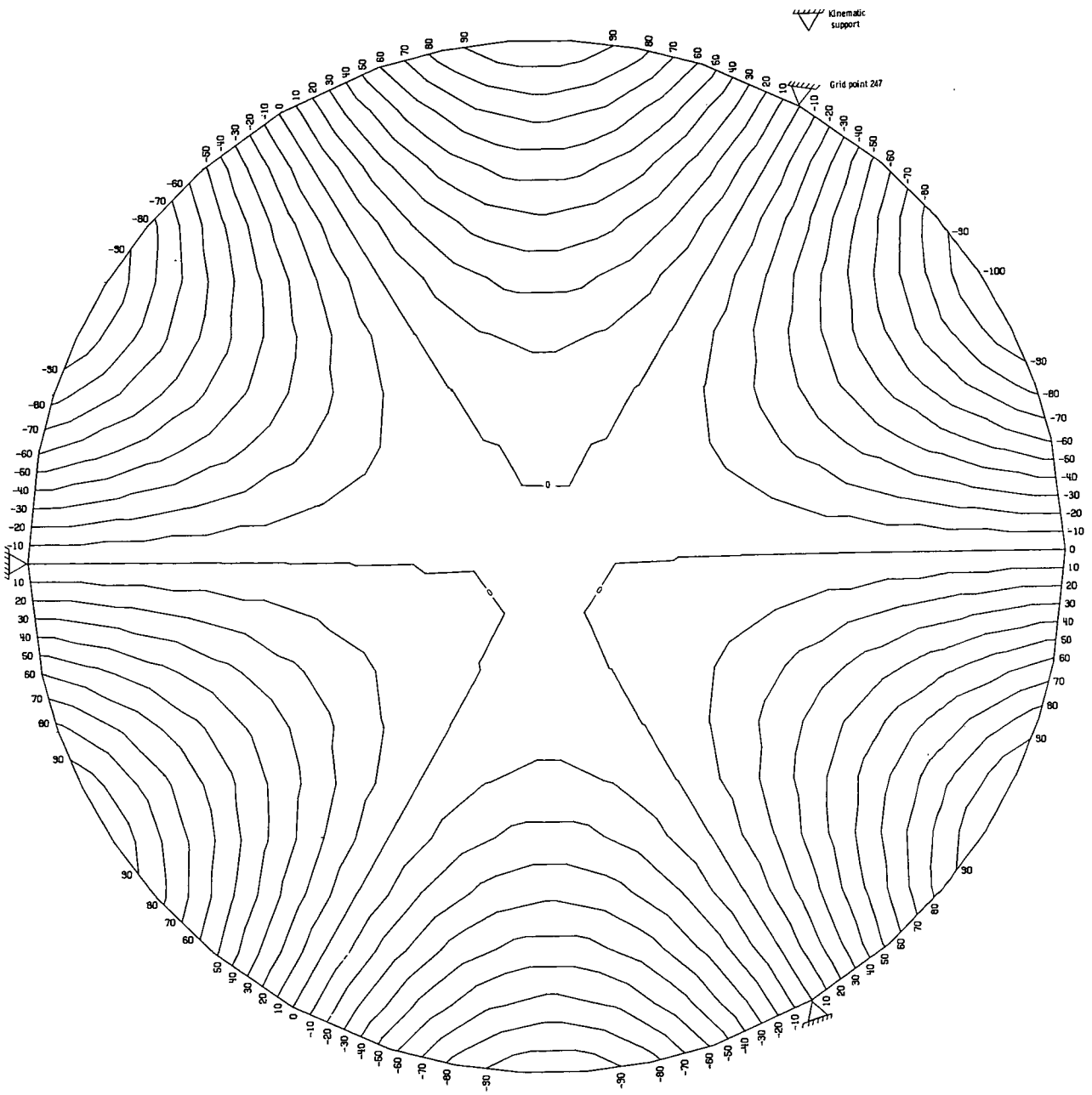

(e) Mode 5.

Figure 3.- Continued.

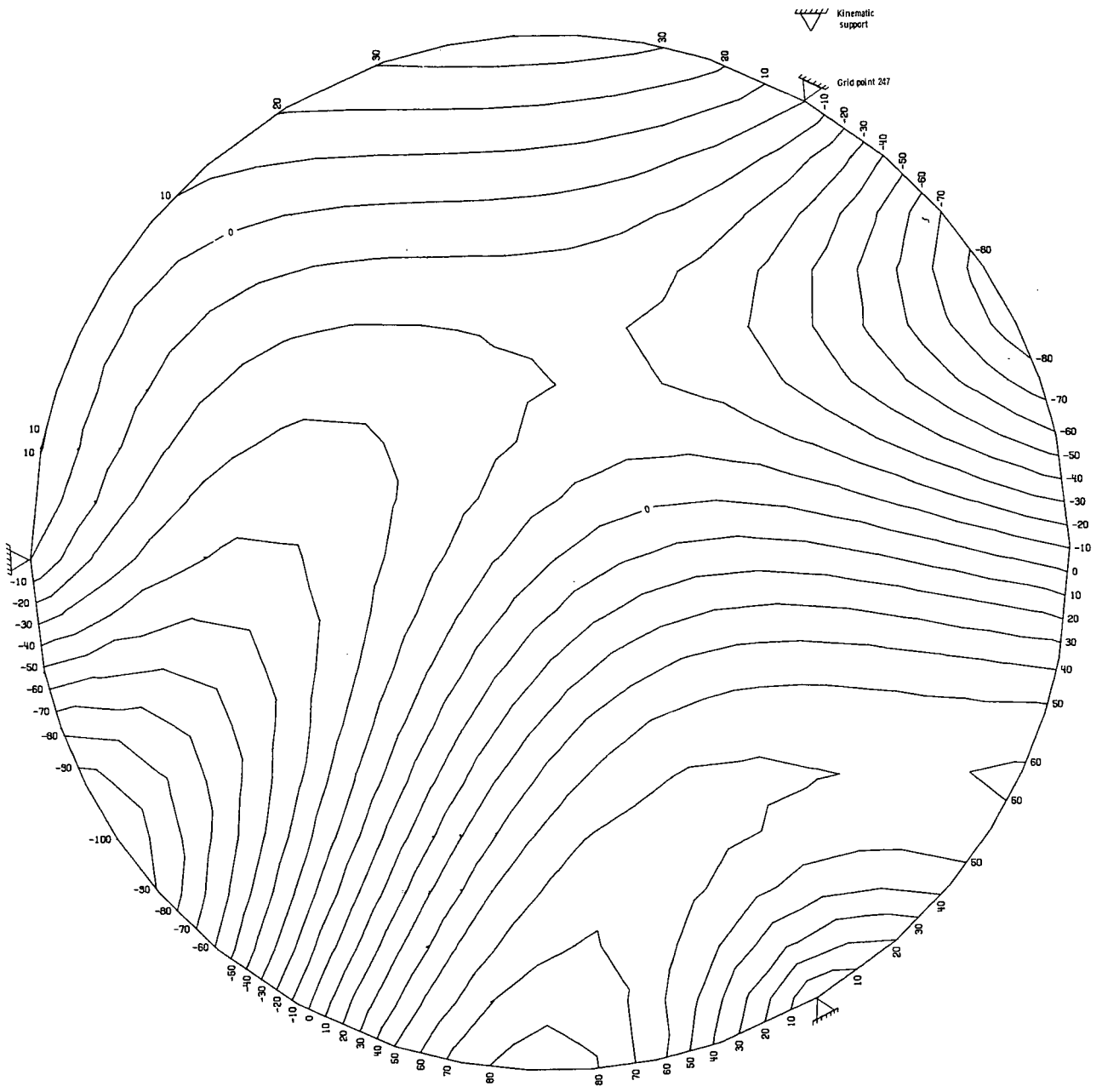

(f) Mode 6.

Figure 3.- Continued.

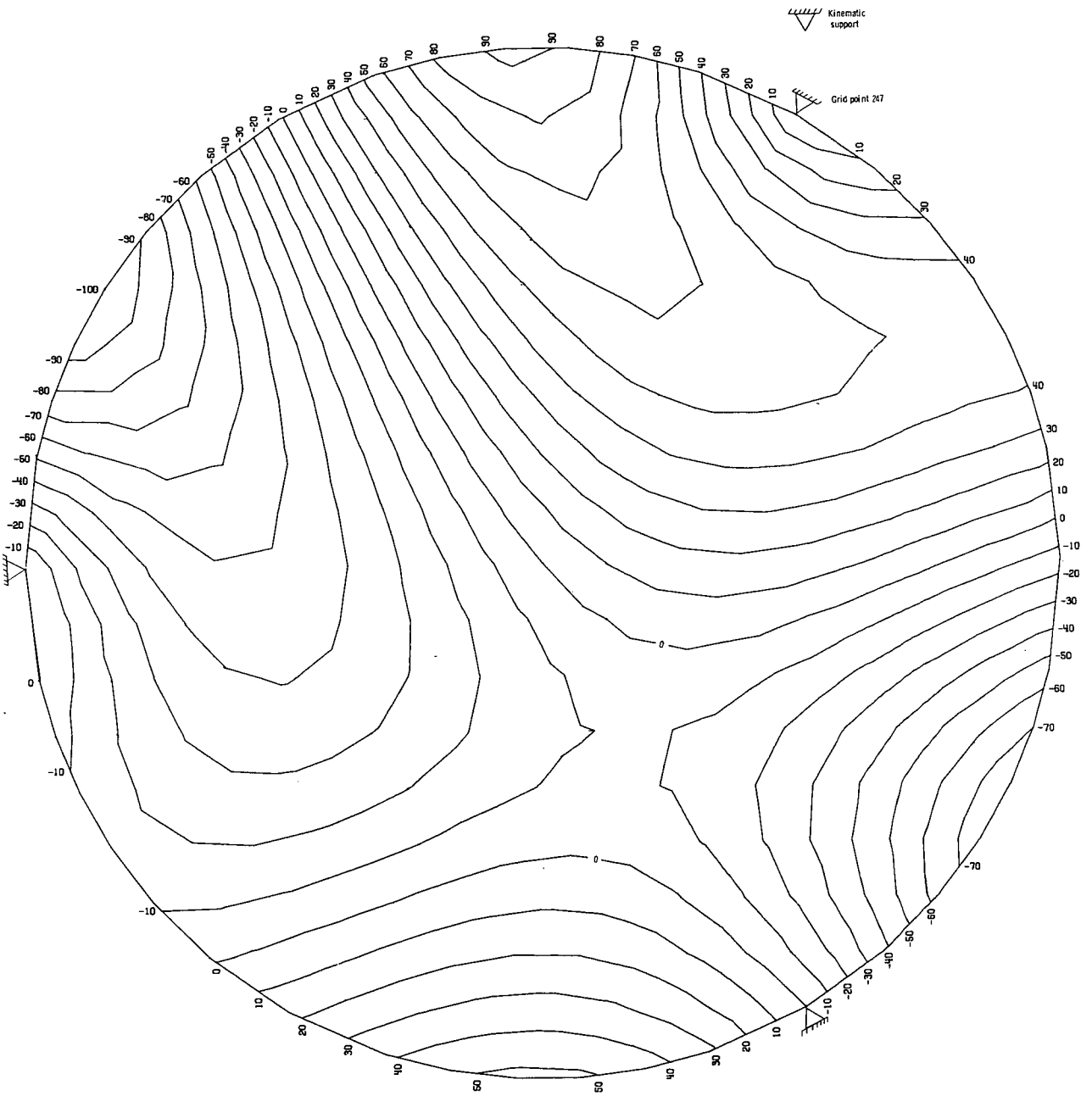

(g) Mode 7.

Figure 3.- Continued.

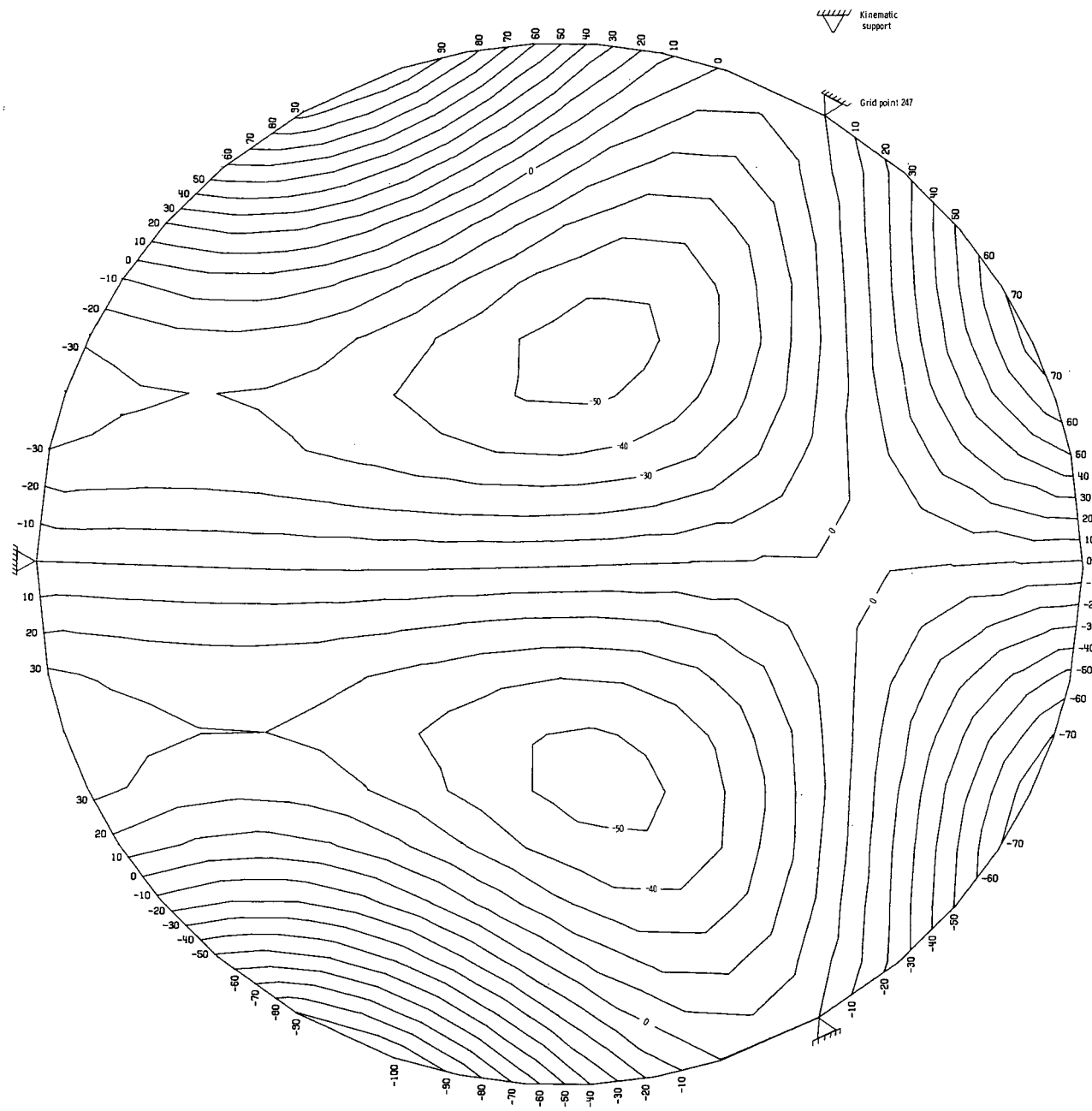

(h) Mode 8.

Figure 3.- Continued.

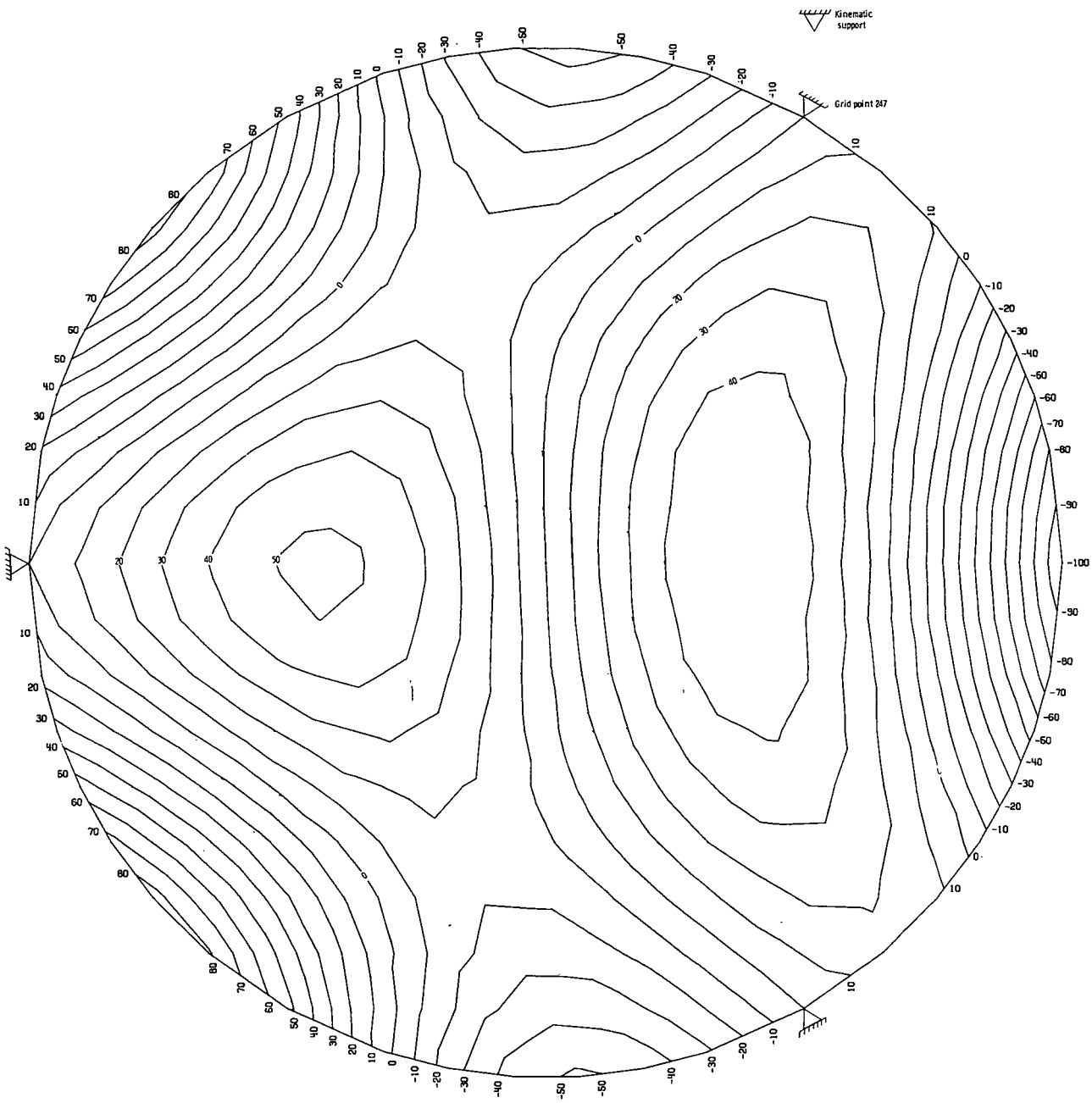

(i) Mode 9.

Figure 3.- Continued.

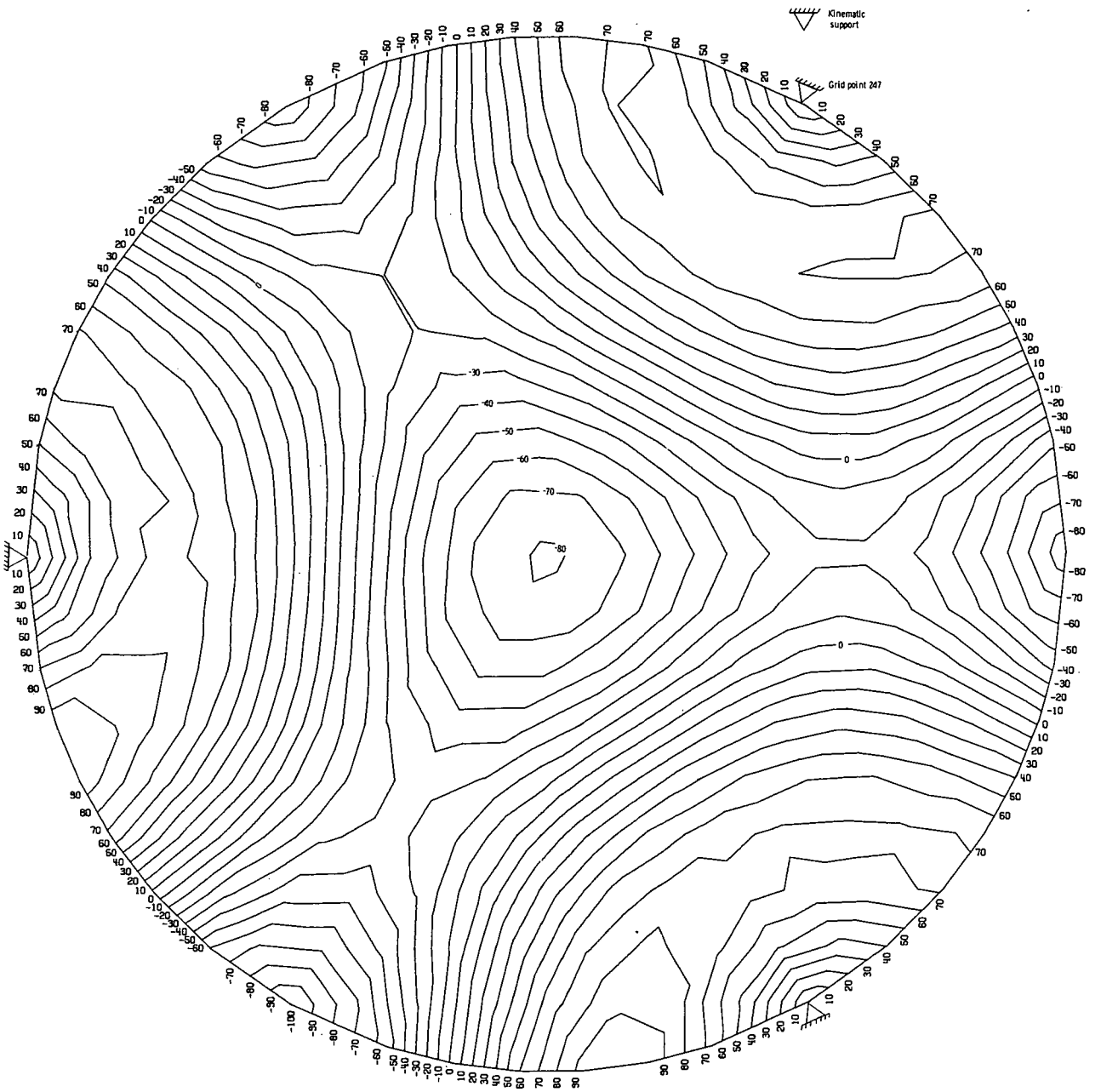

(j) Mode 10.

Figure 3.- Concluded.

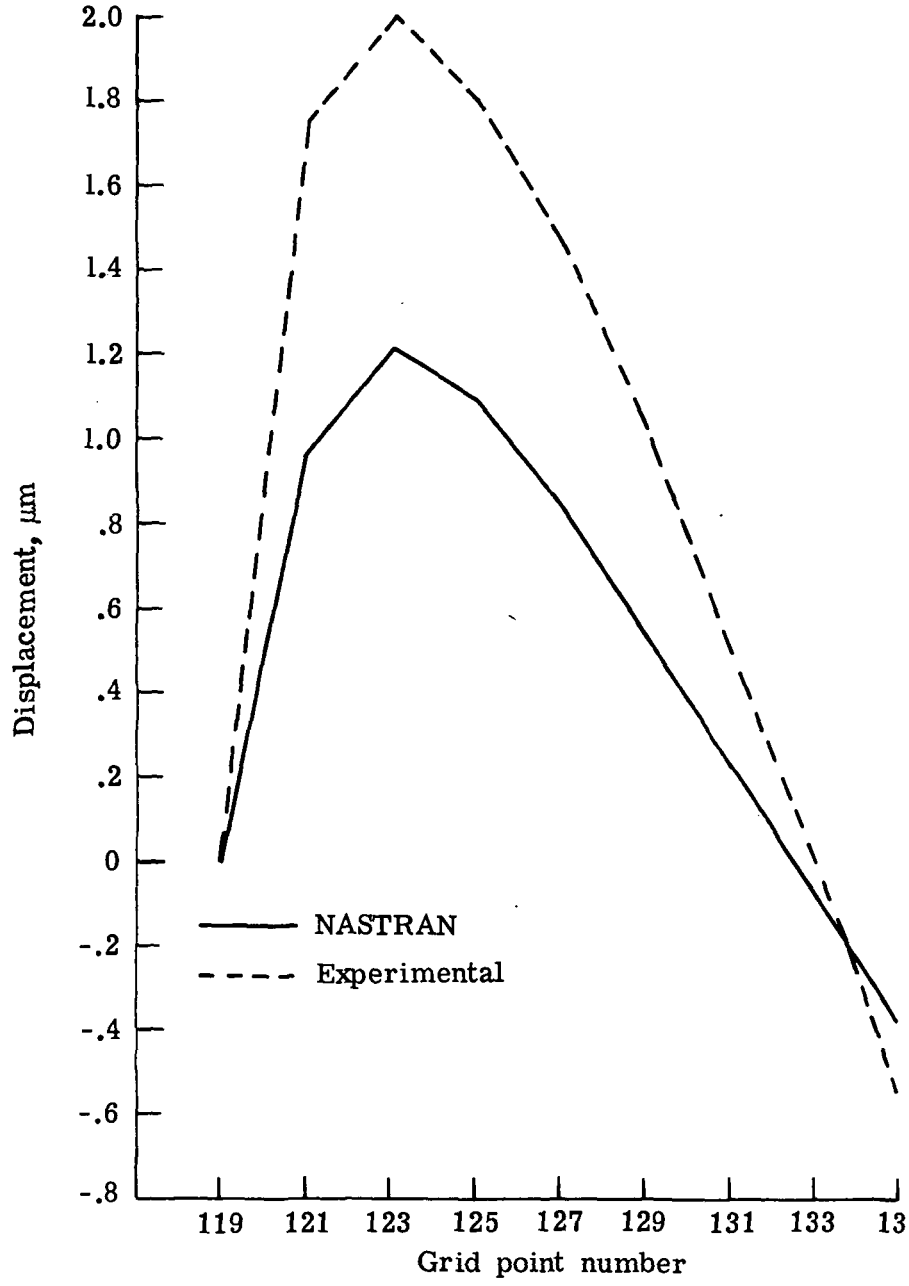

(a) Grid point 121.

Figure 4.- Displacement for normal force of 4.448 N at one grid point.

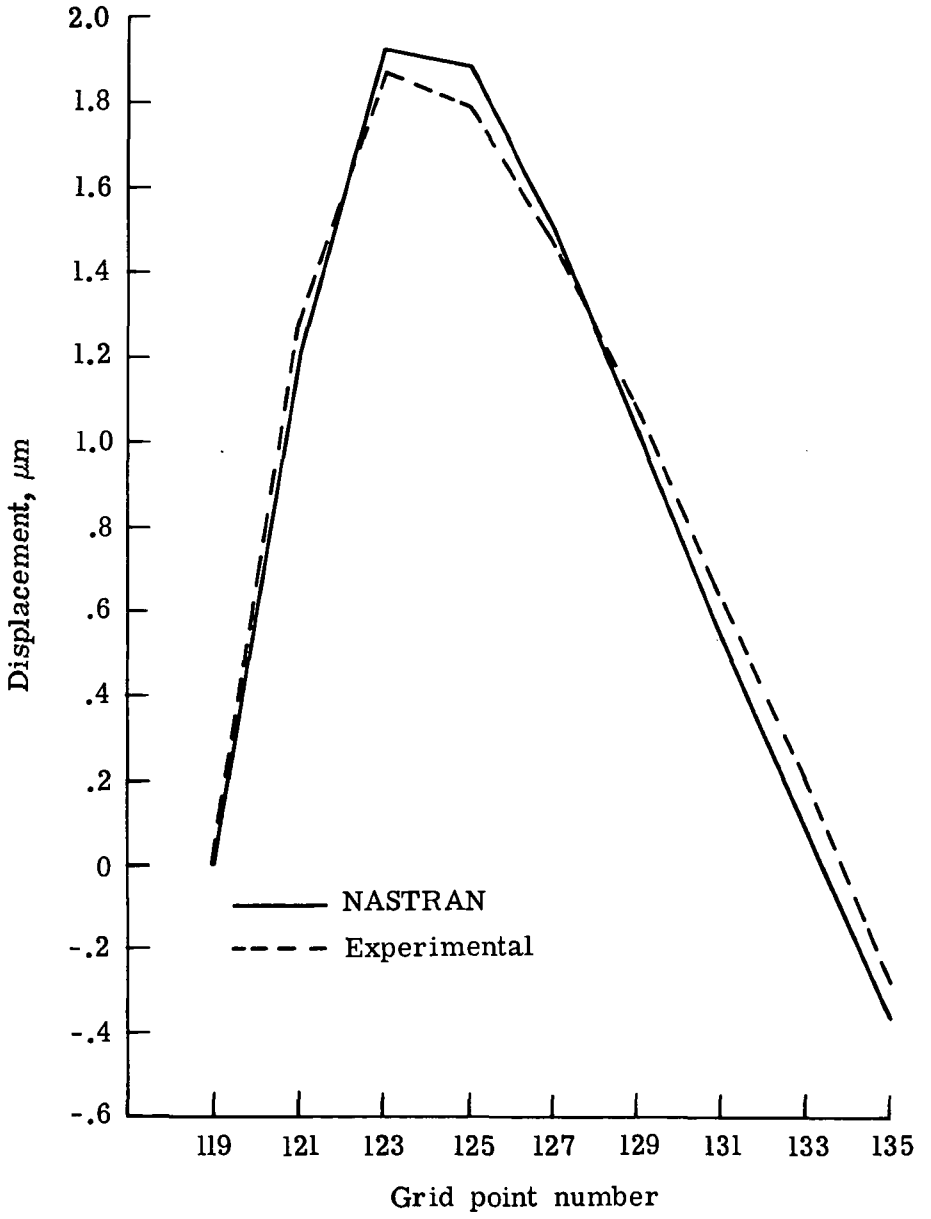

(b) Grid point 123.

Figure 4.- Continued.

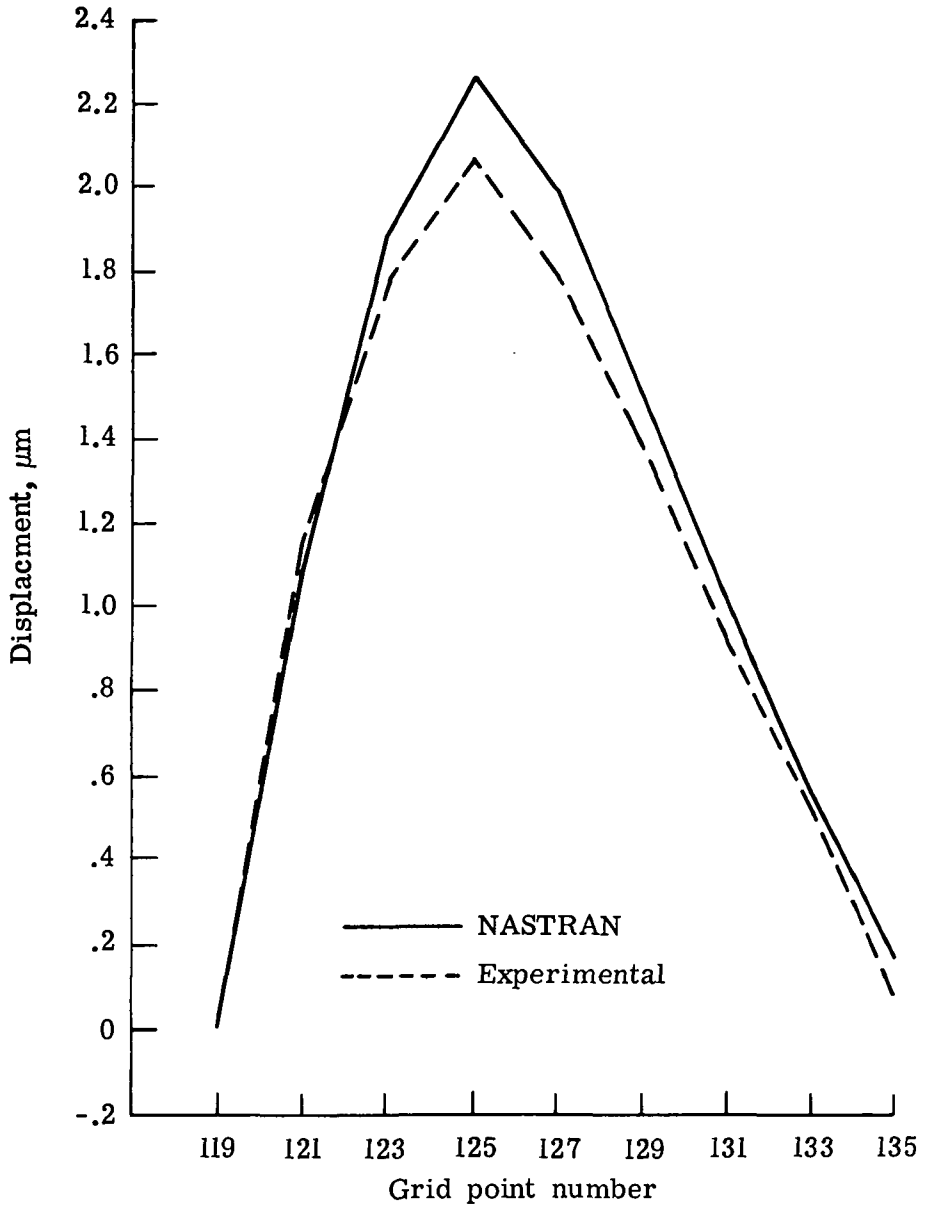

(c) Grid point 125.

Figure 4.- Continued.

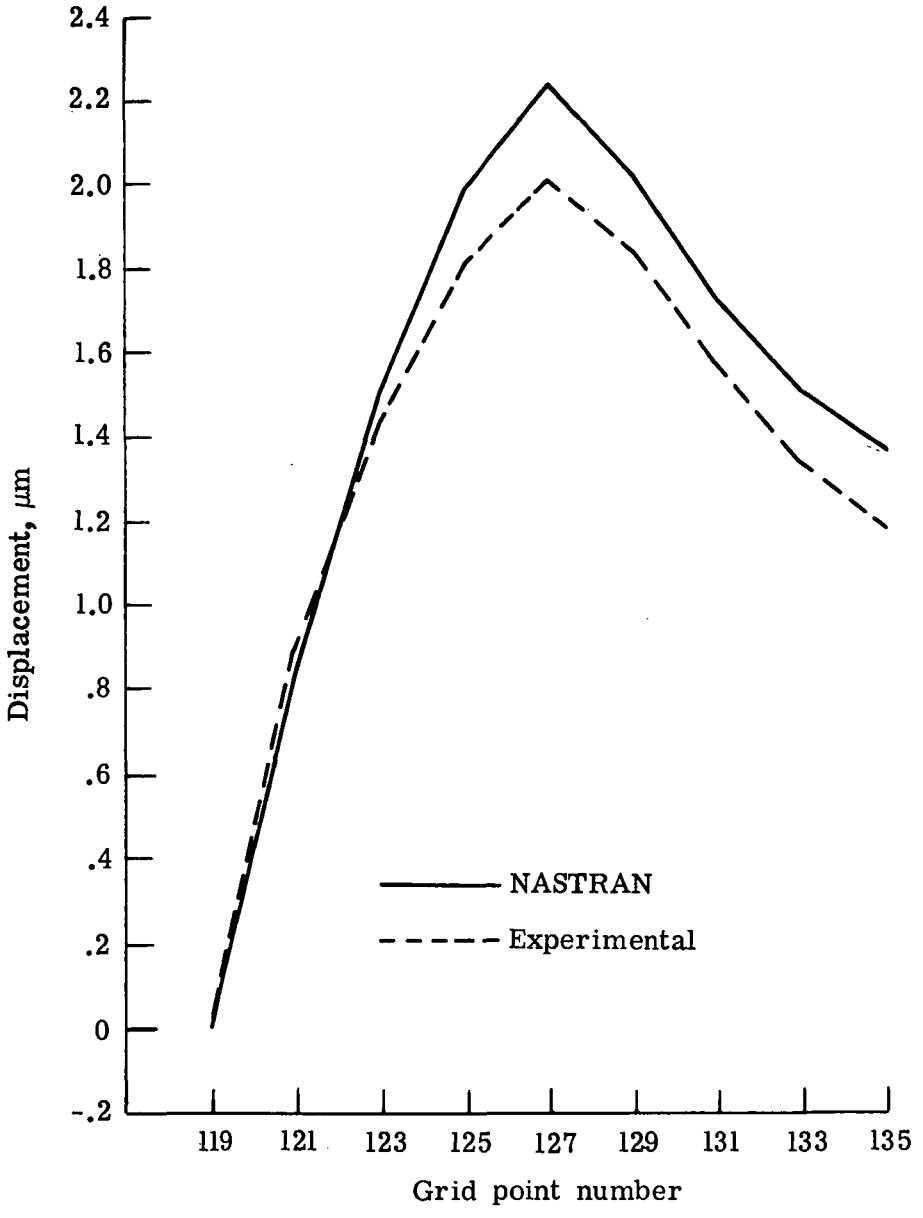

(d) Grid point 127.

Figure 4.- Continued.

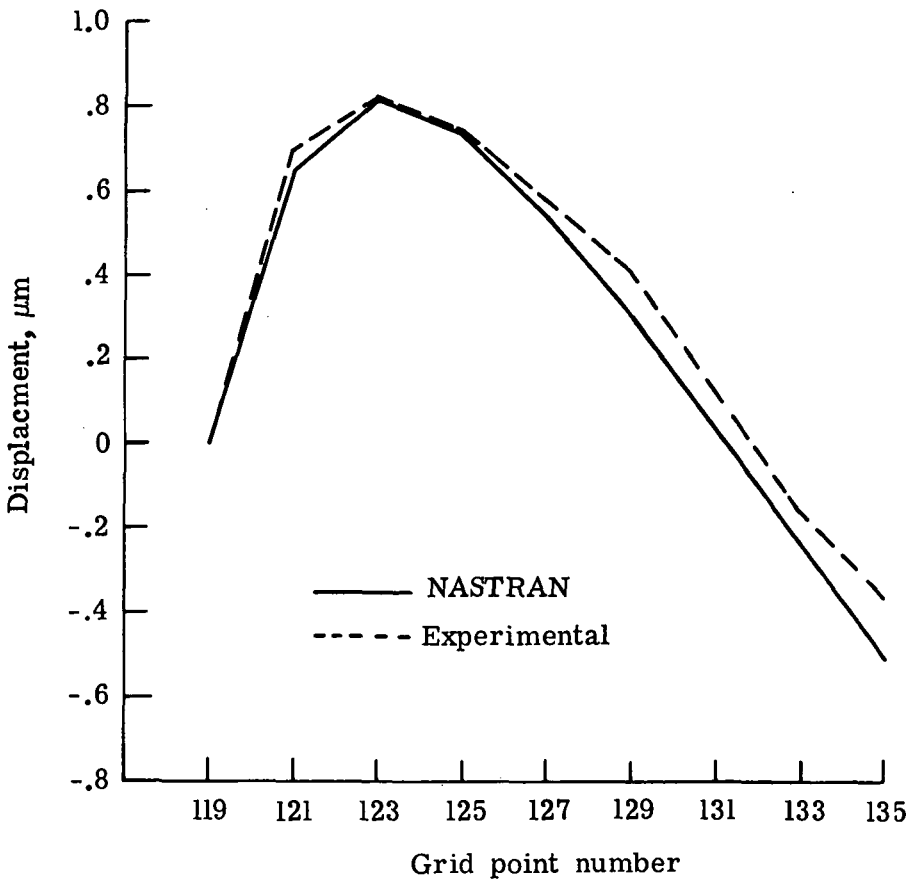

(e) Grid point 153.

Figure 4.- Continued.

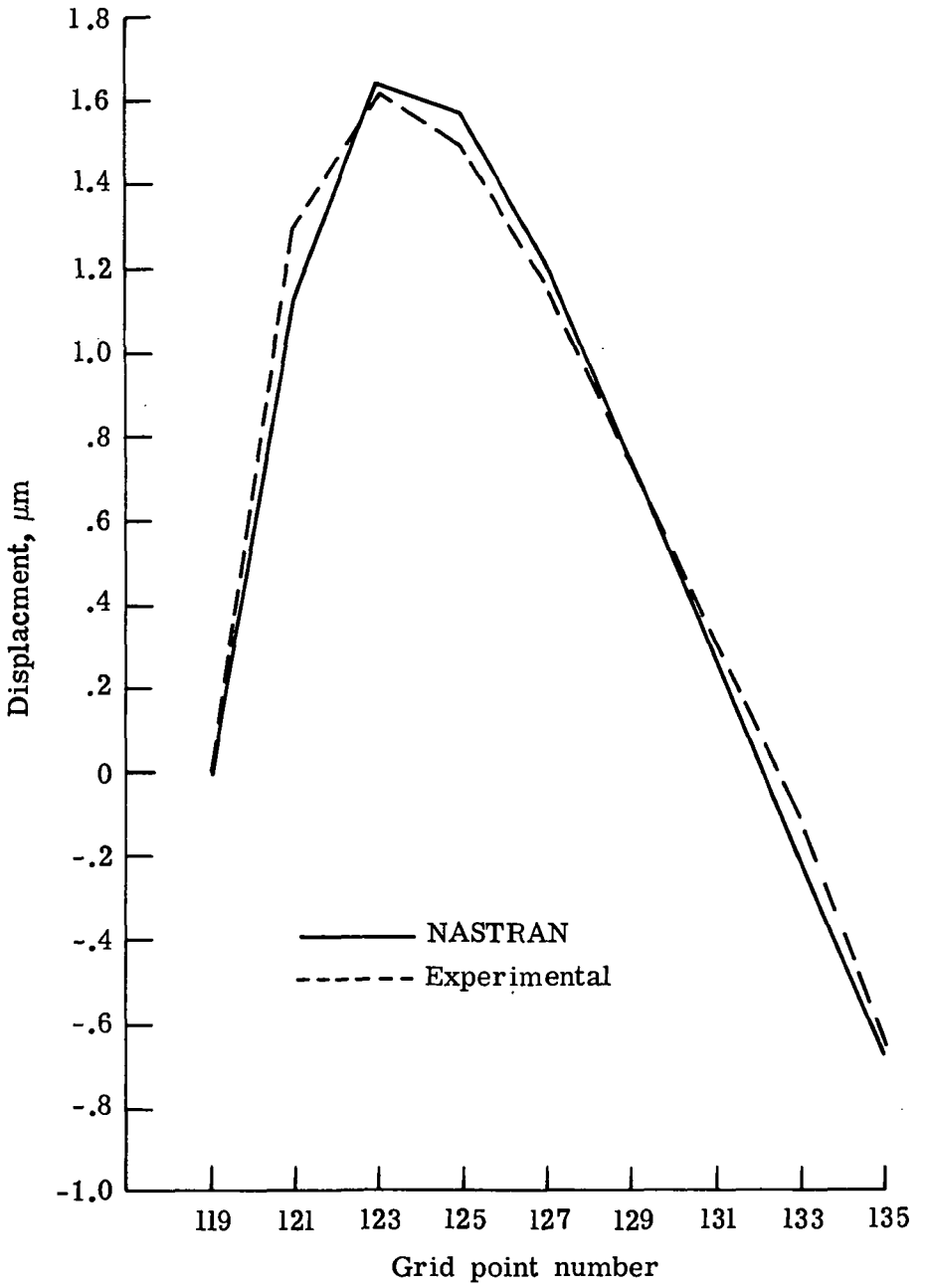

(f) Grid point 155.

Figure 4.- Continued.

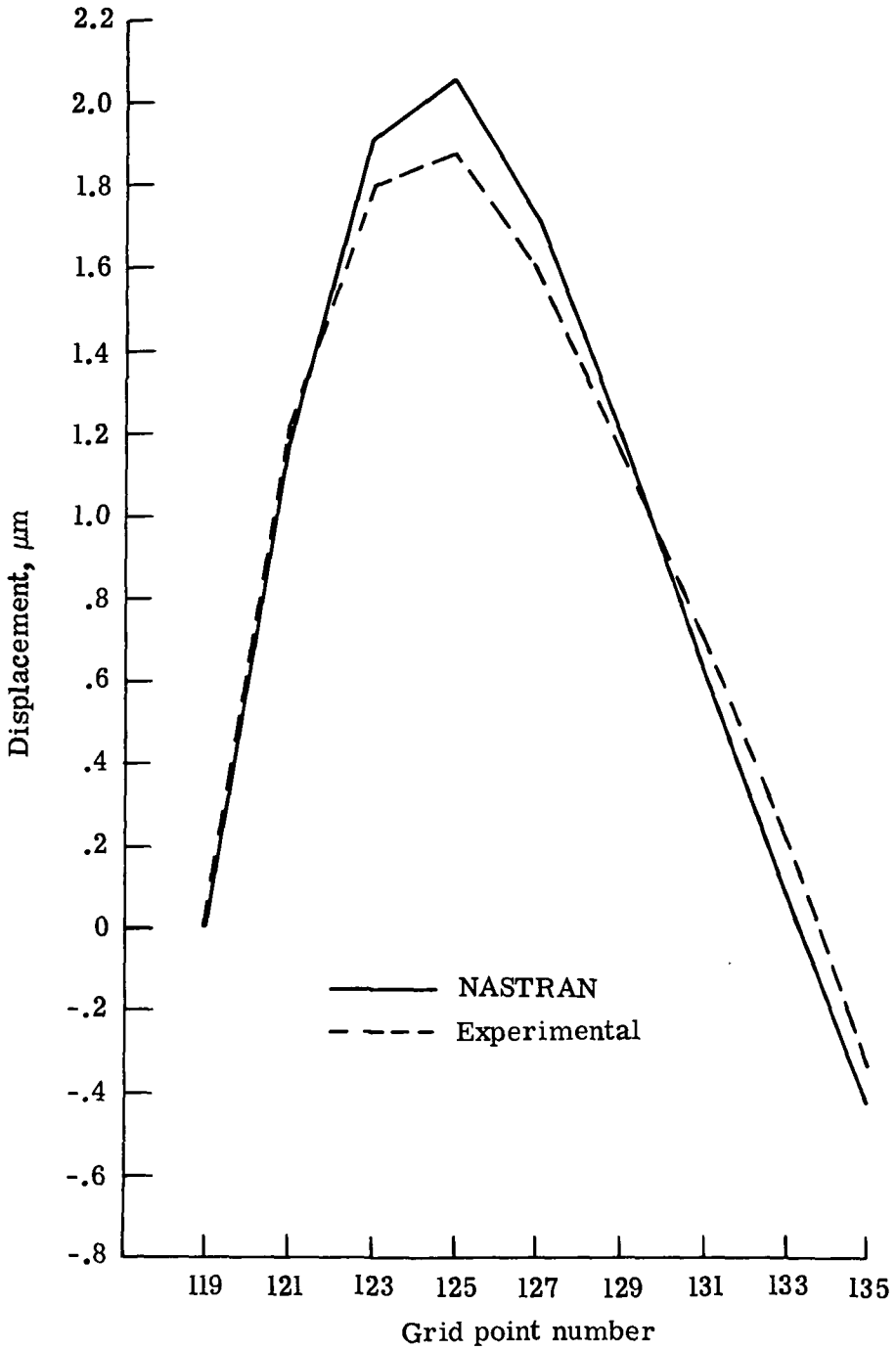

(g) Grid point 157.

Figure 4.- Continued.

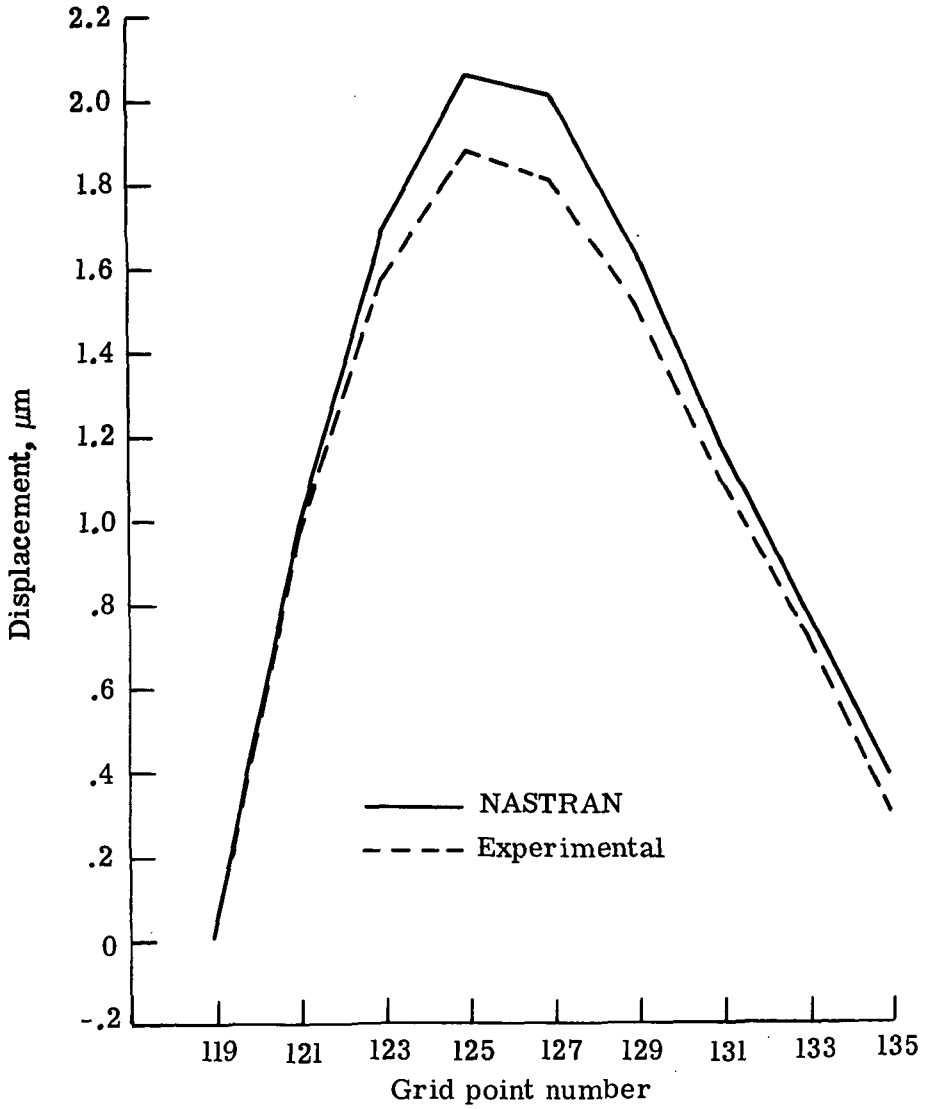

(h) Grid point 159.

Figure 4.- Continued.

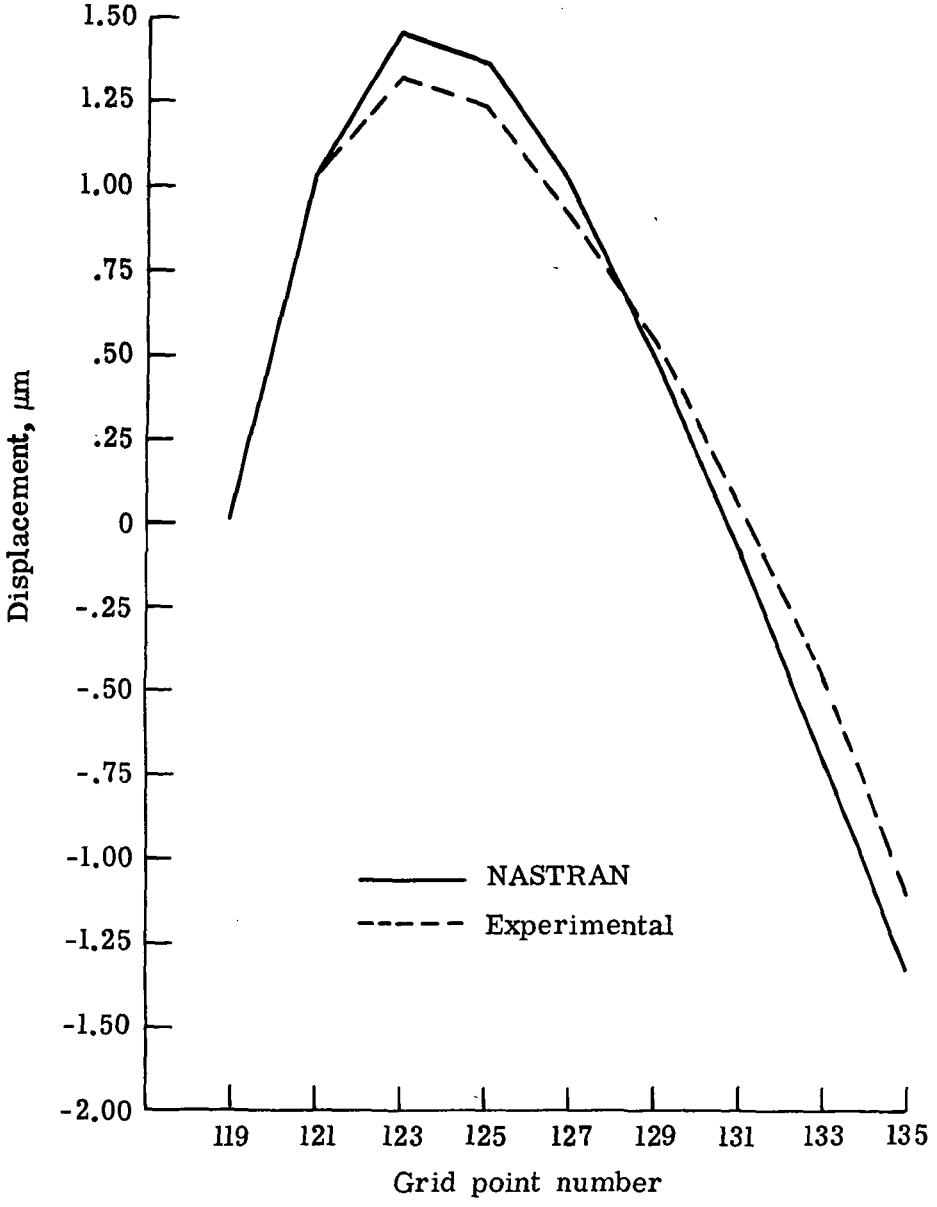

(i) Grid point 186.

Figure 4.- Continued.

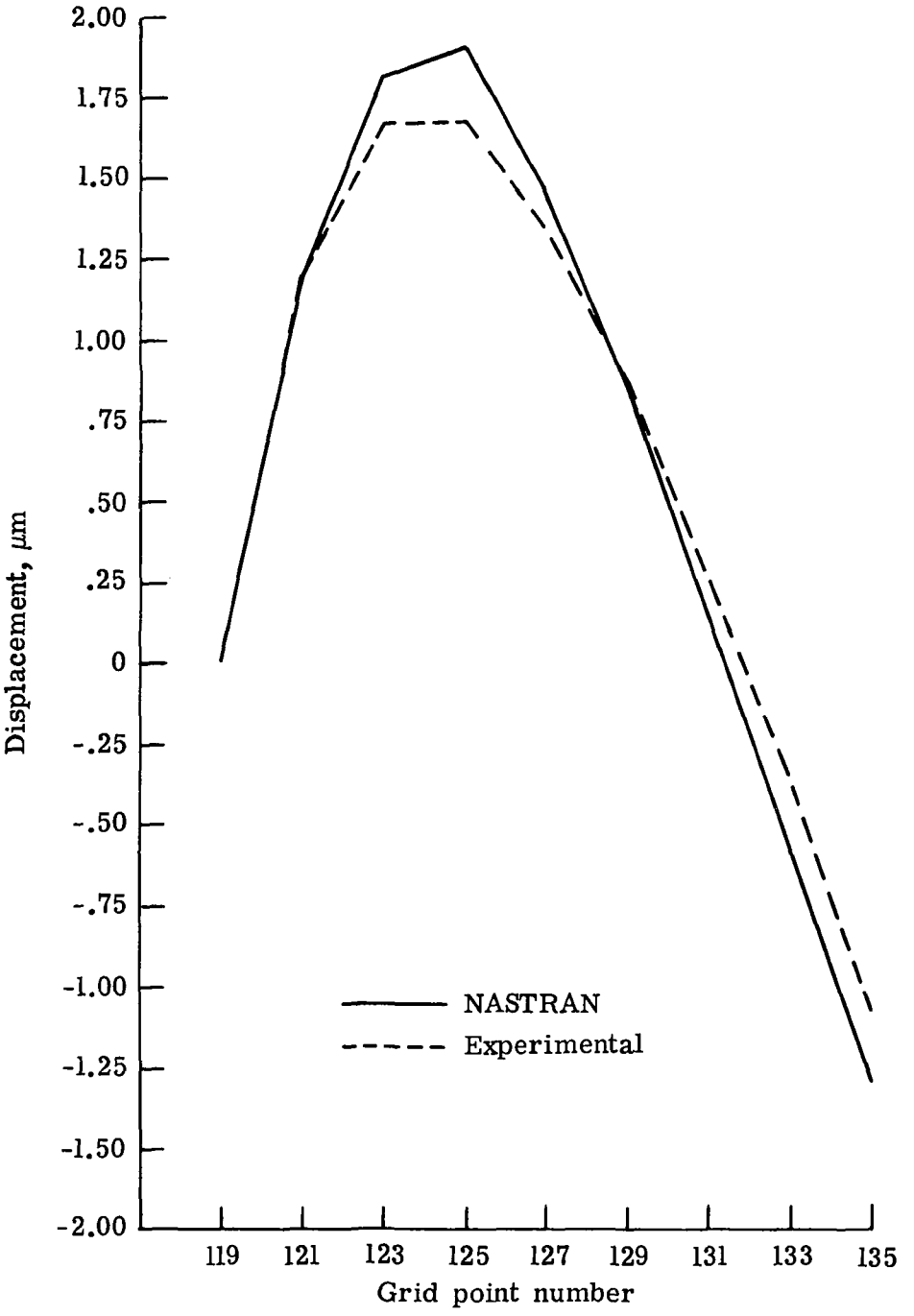

(j) Grid point 188.

Figure 4.- Continued.

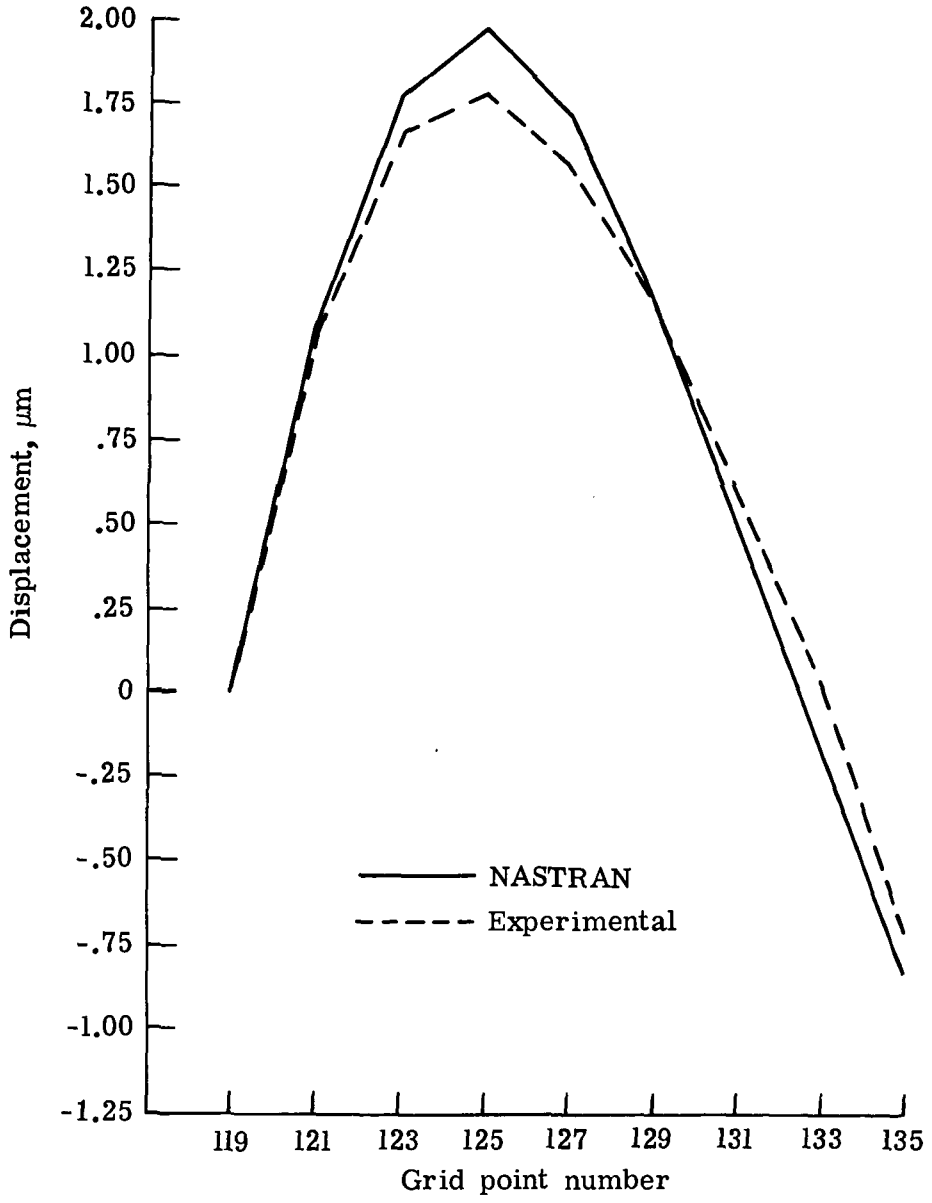

(k) Grid point 190.

Figure 4.- Continued.

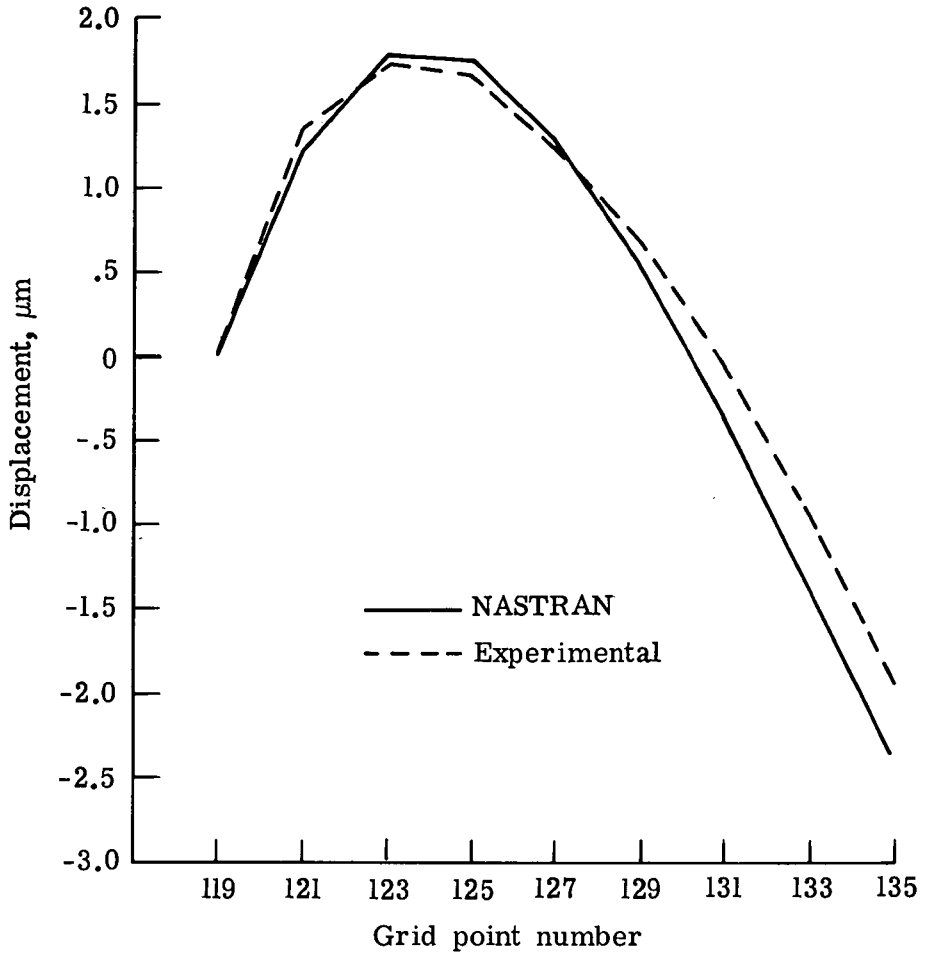

(*l*) Grid point 215.

Figure 4.- Continued.

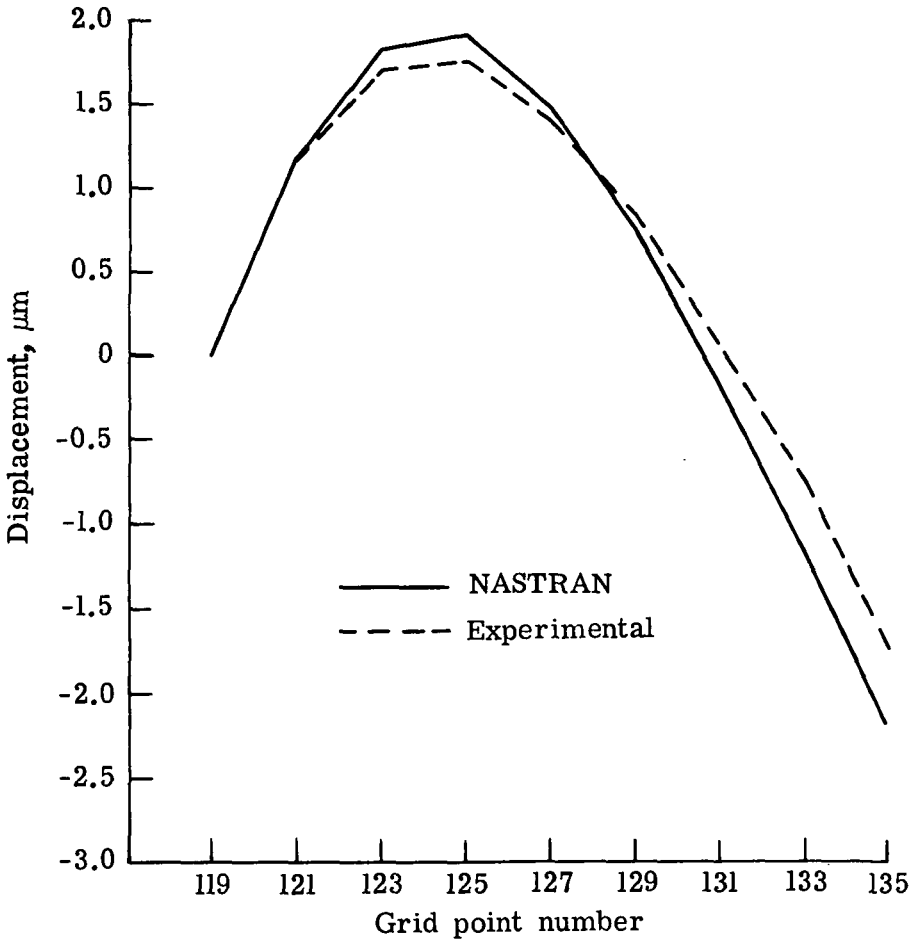

(m) Grid point 217.

Figure 4.- Continued.

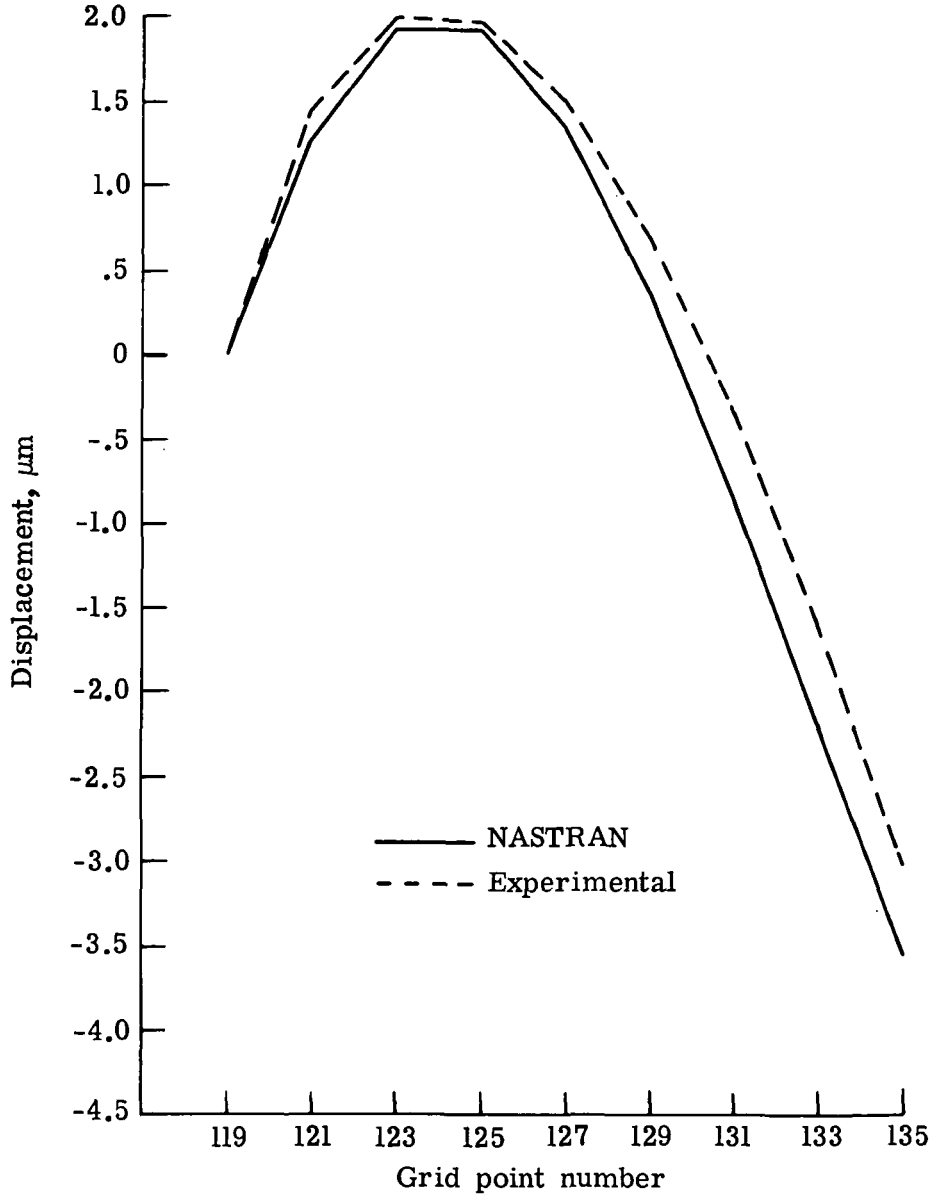

(n) Grid point 239.

Figure 4.- Concluded.

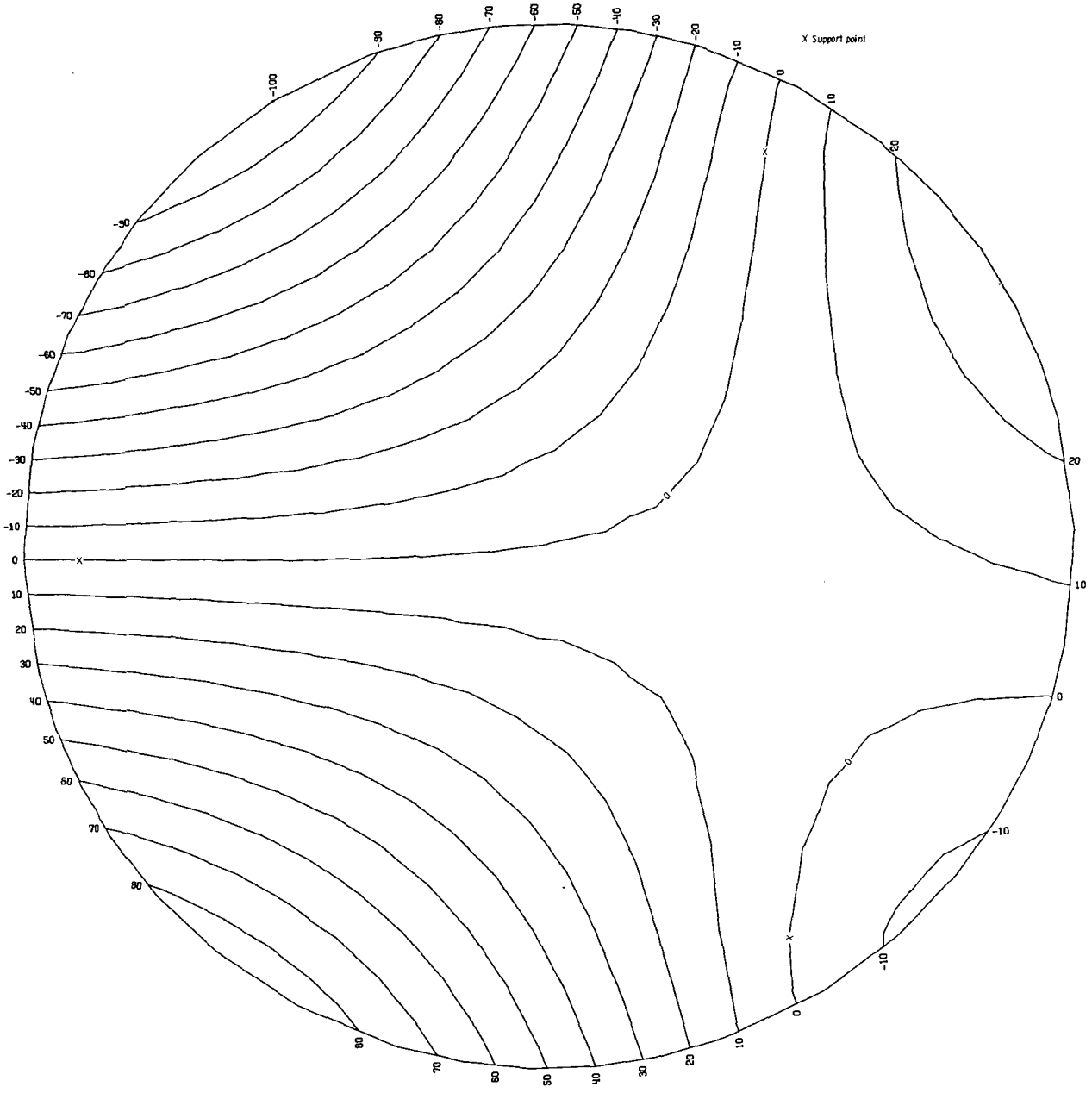

(a) Mode 1.

Figure 5.- Contour plot for 0.762-meter-diameter solid spherical mirror with 60-to-1 diameter-to-thickness ratio and supports moved to grid points 25, 120, and 236.

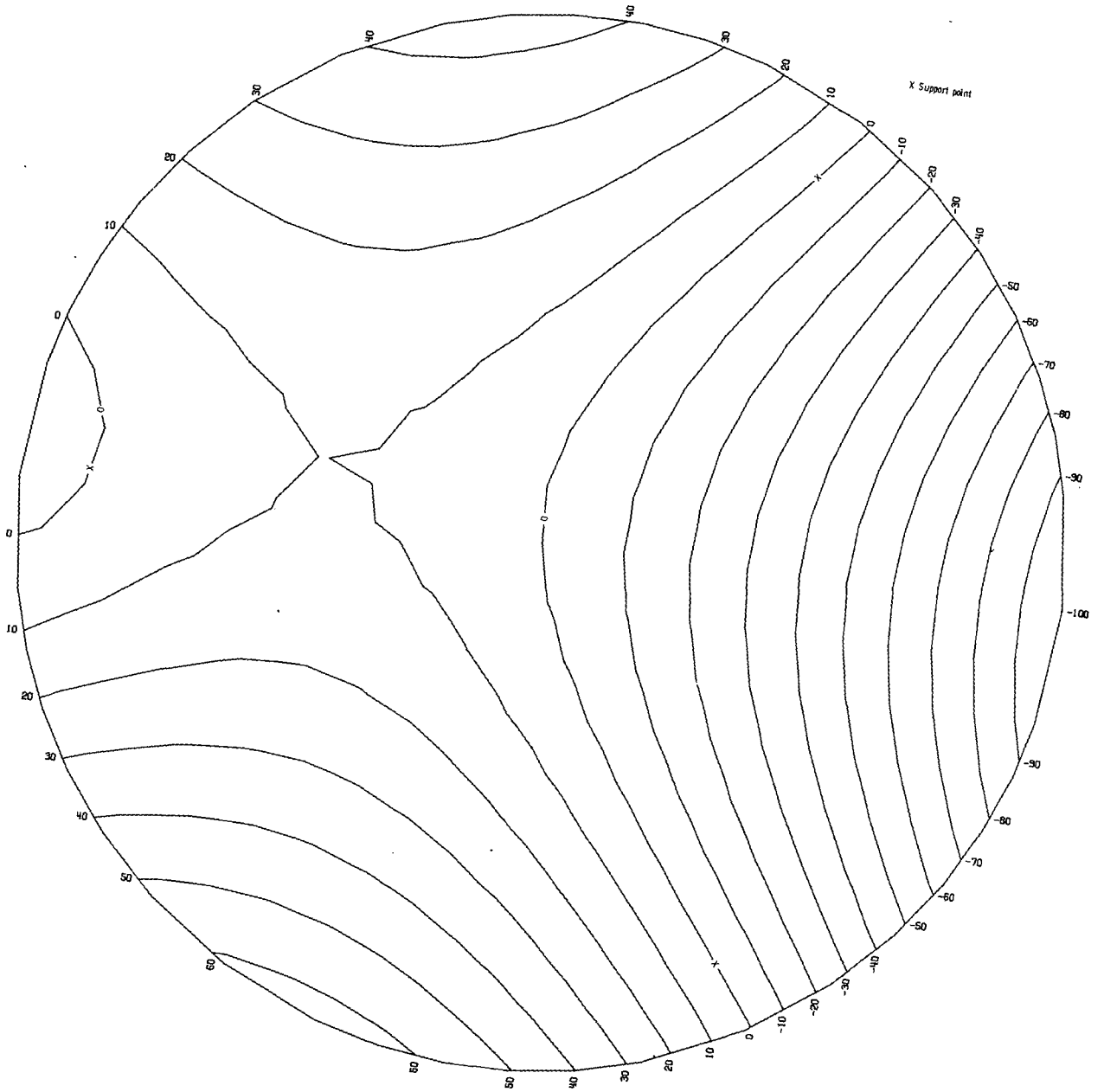

(b) Mode 2.

Figure 5.- Continued.

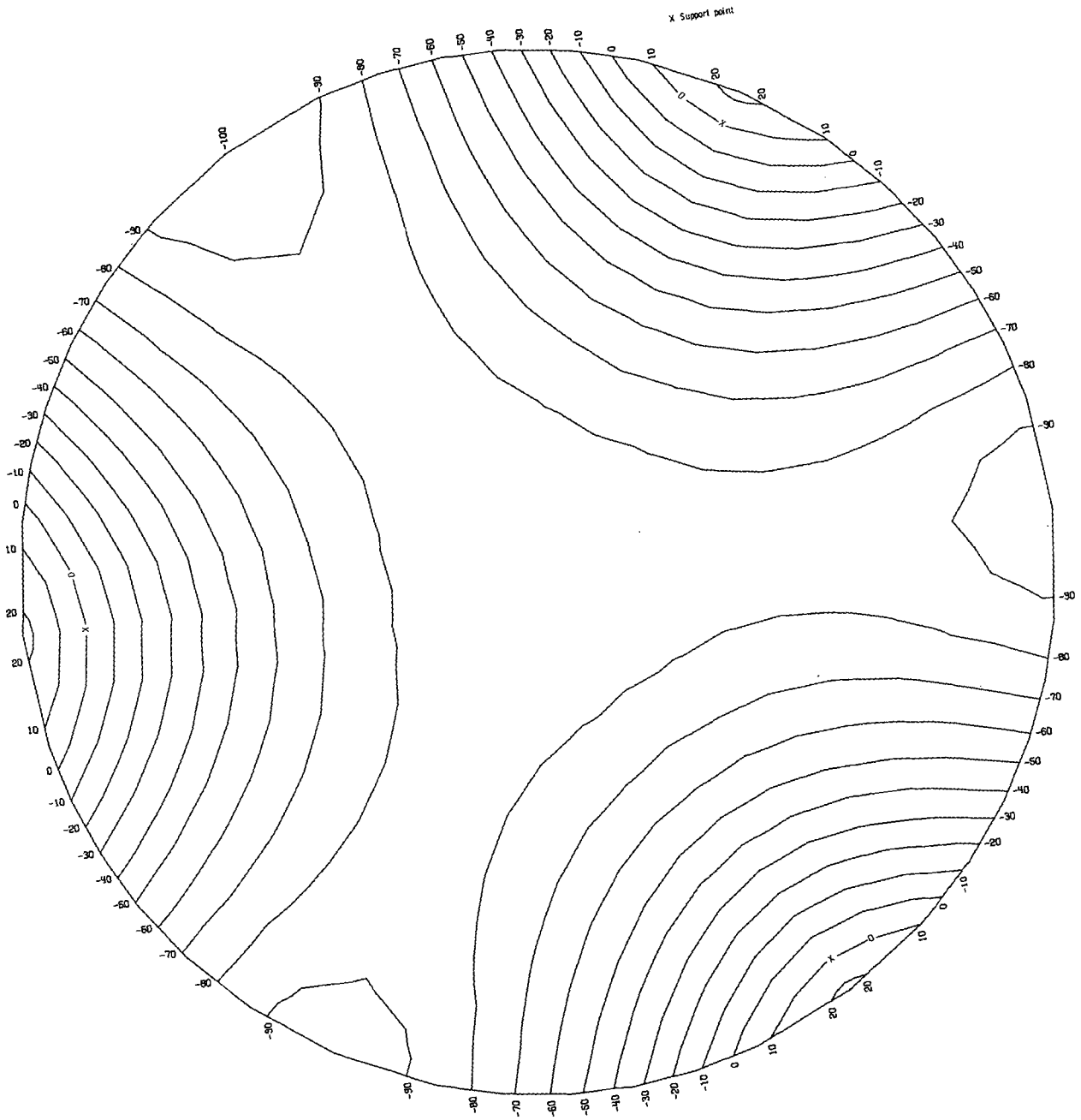

(c) Mode 3.

Figure 5.- Continued.

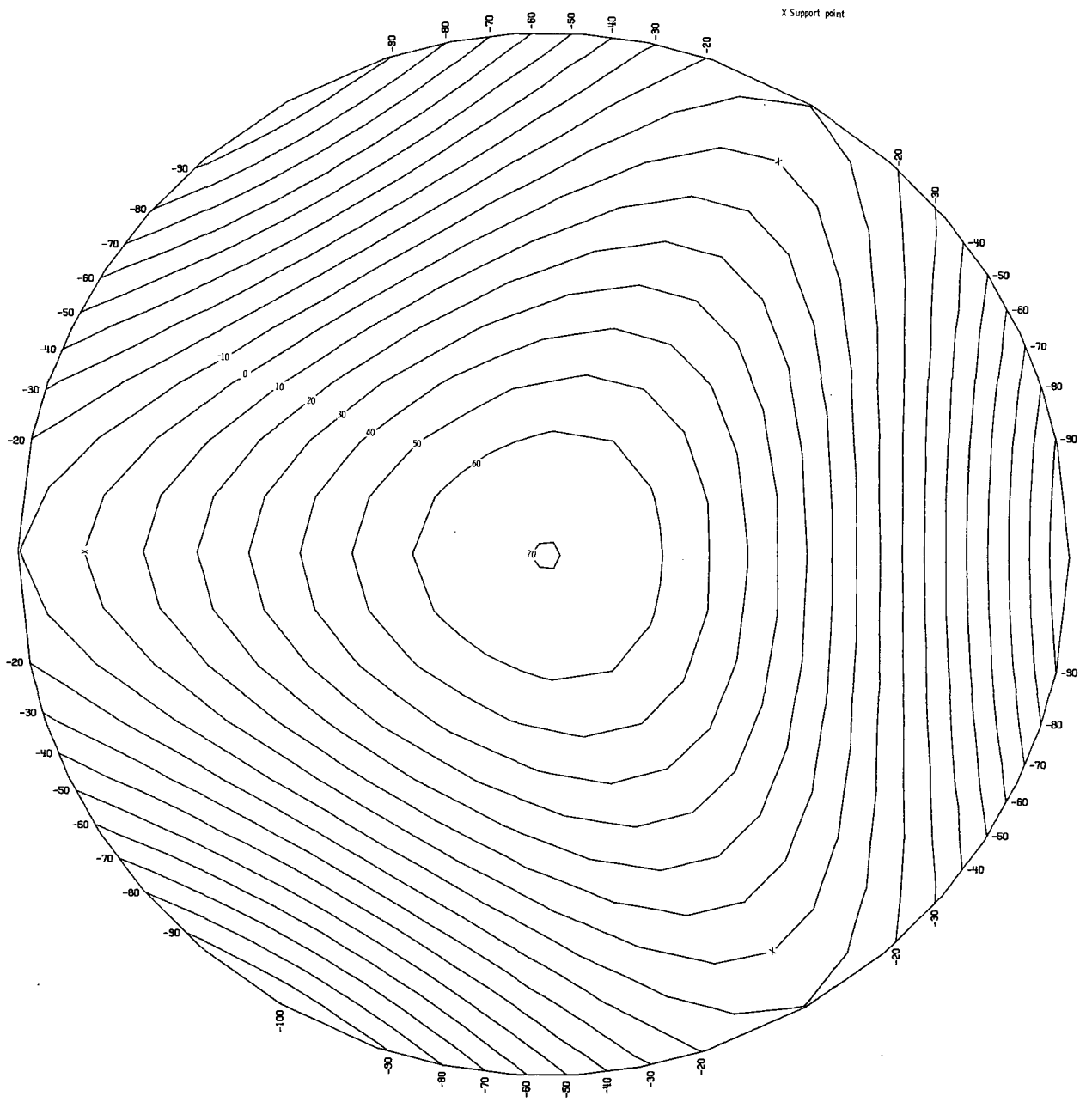

(d) Mode 4.

Figure 5.- Continued.

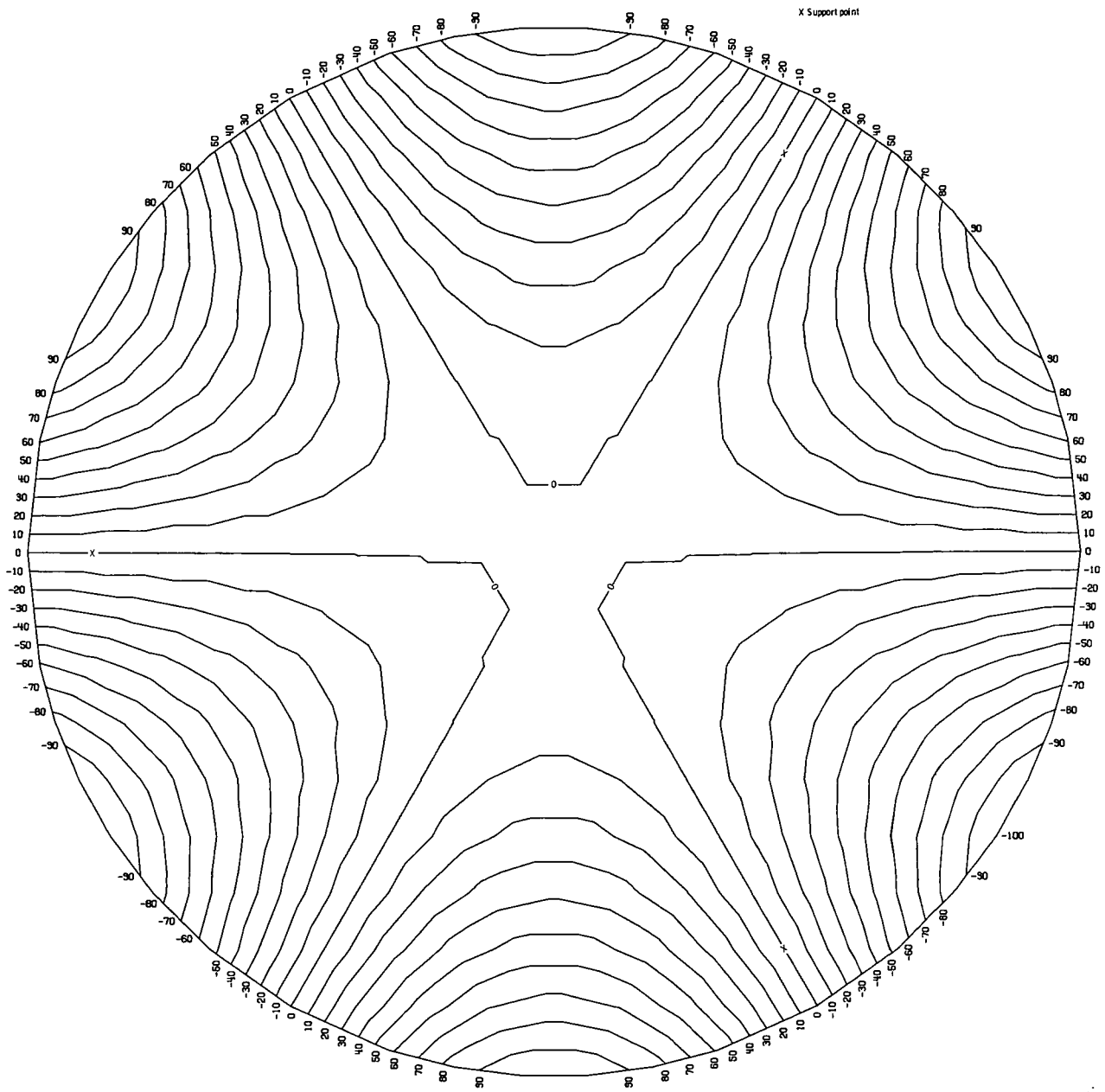

(e) Mode 5.

Figure 5.- Continued.

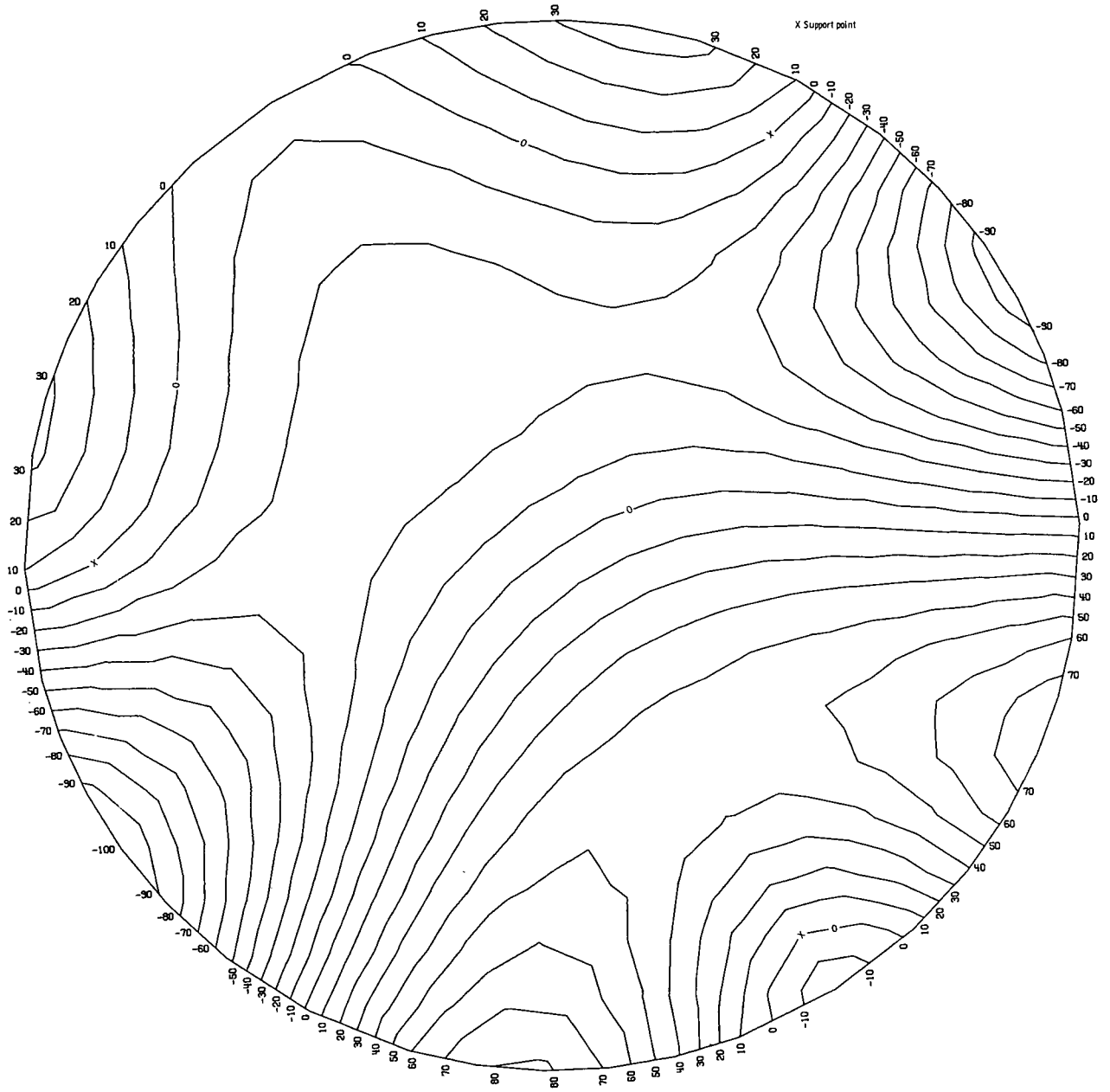

(f) Mode 6.

Figure 5.- Continued.

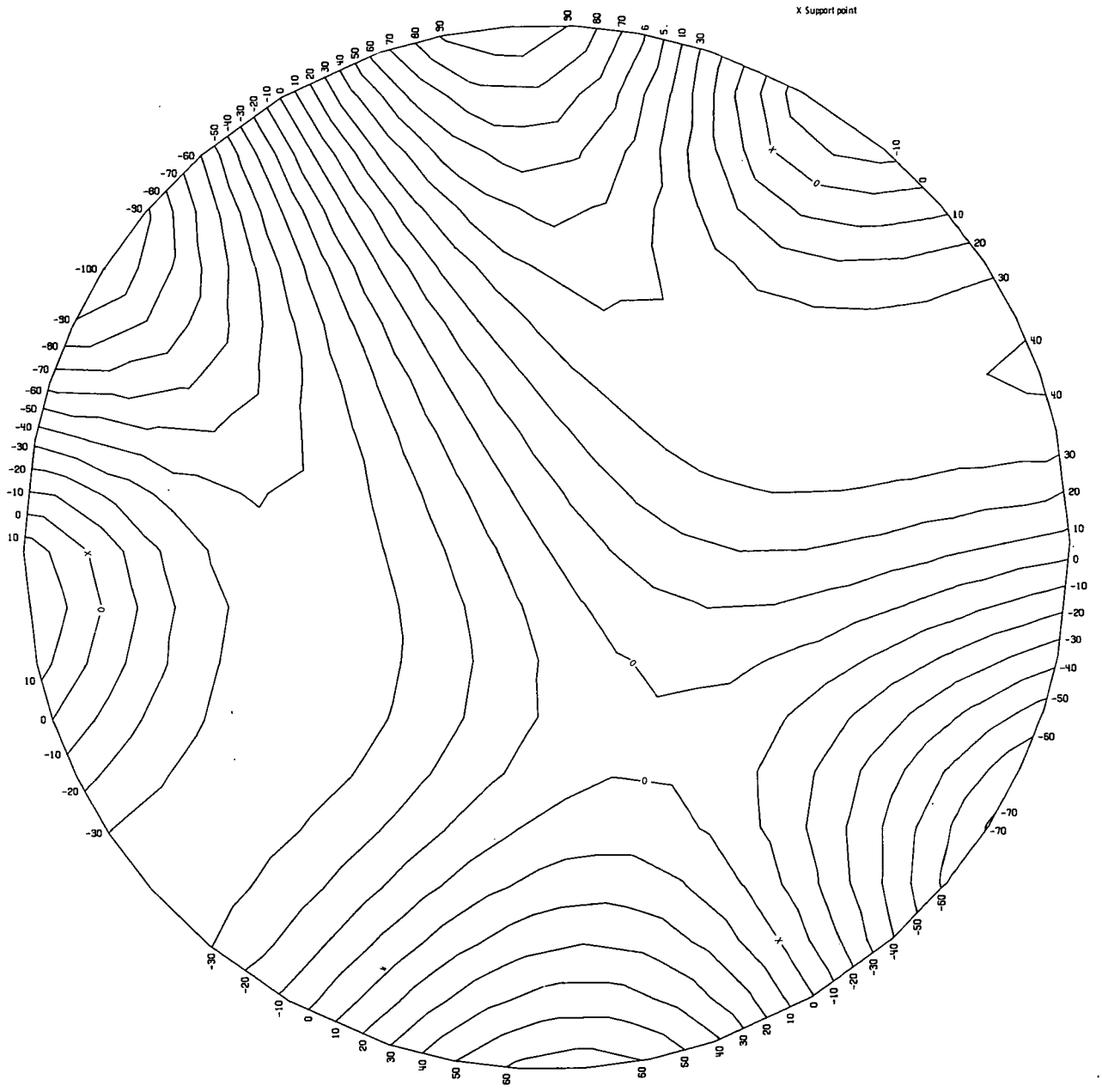

(g) Mode 7.

Figure 5.- Concluded.

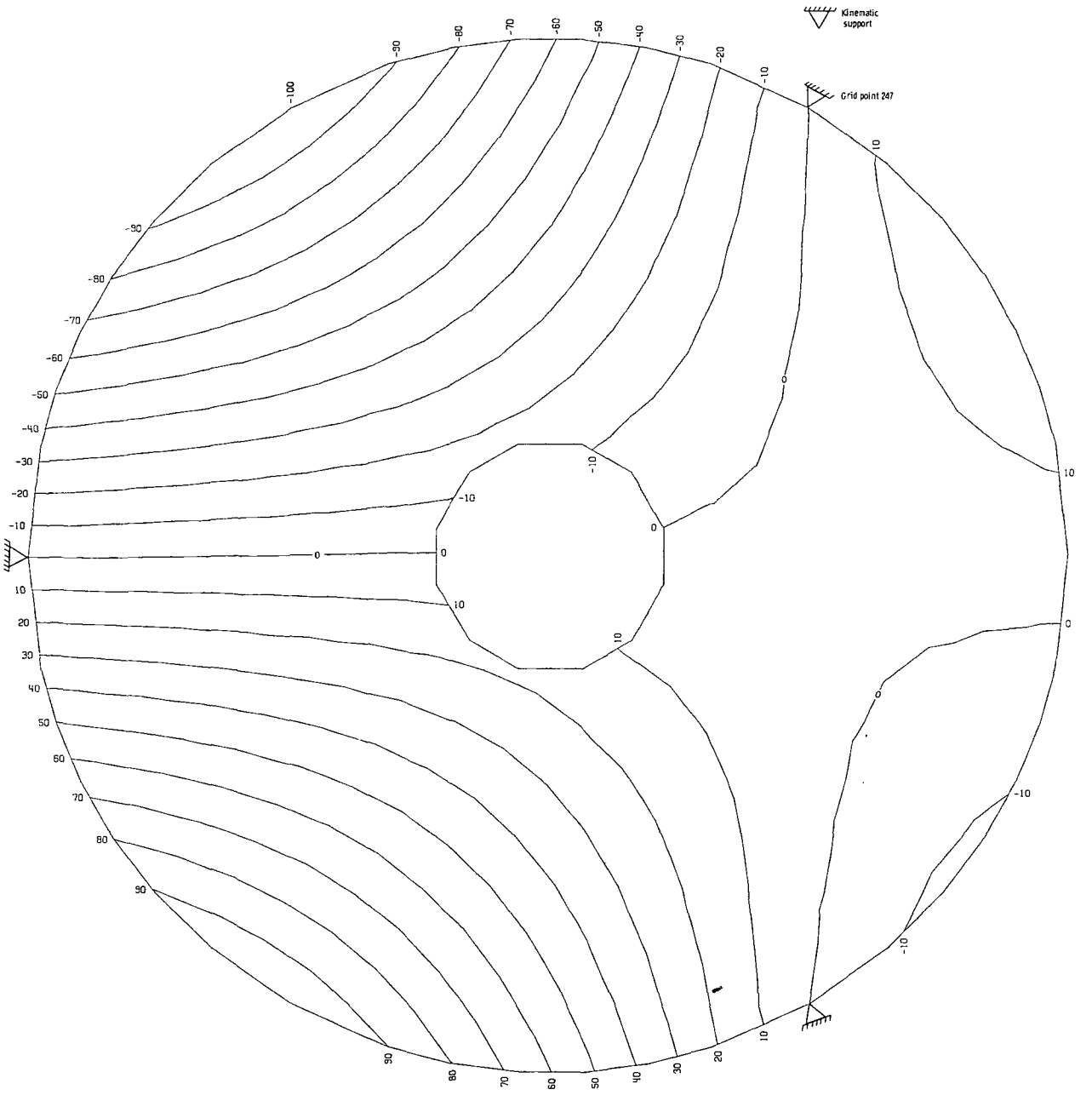

(a) Mode 1.

Figure 6.- Contour plot for 0.762-meter-diameter spherical mirror with 60-to-1 diameter-to-thickness ratio and central hole that is 22 percent of outside diameter with supports at grid points 15, 119, and 247.

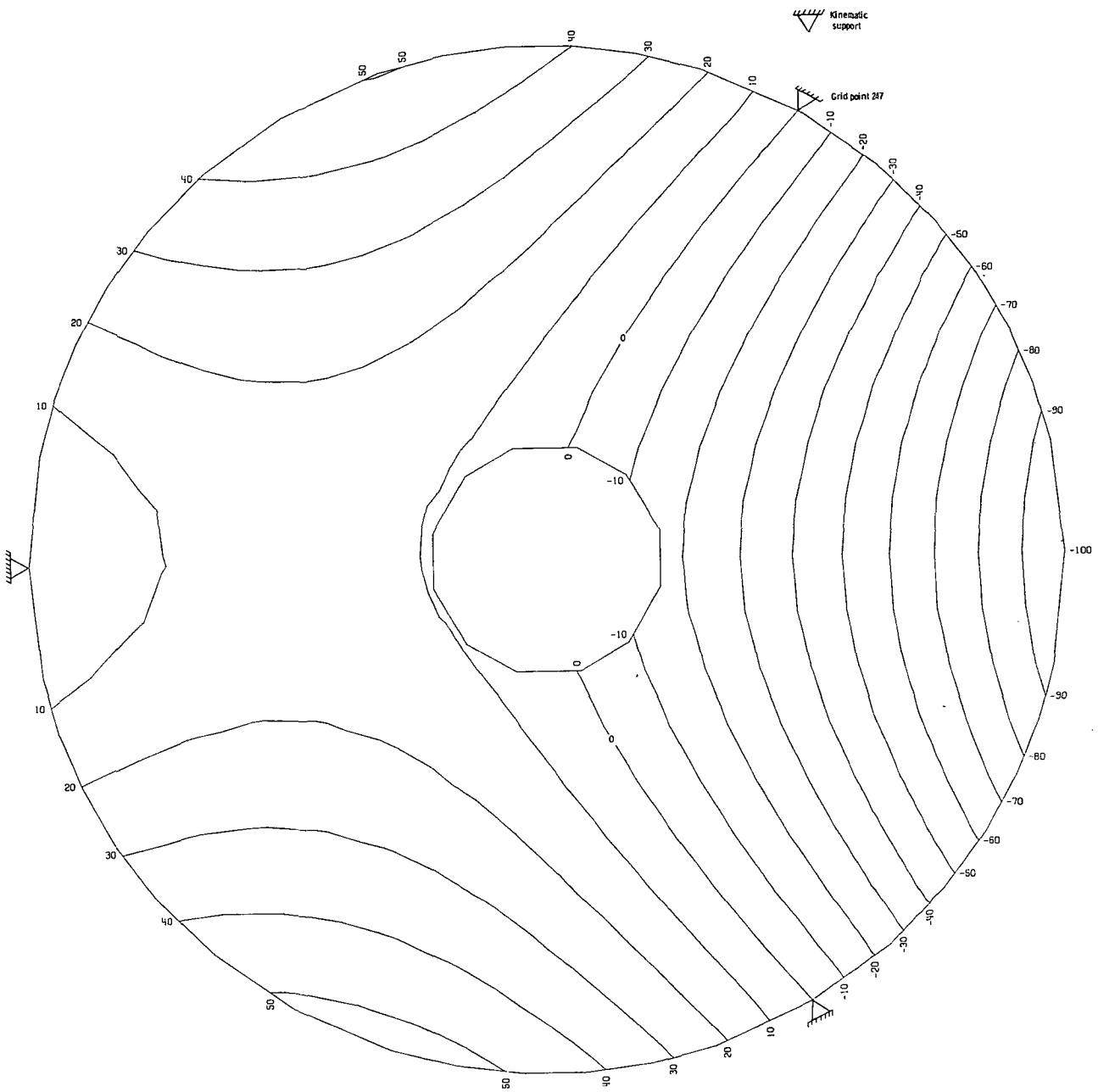

(b) Mode 2.

Figure 6.- Continued.

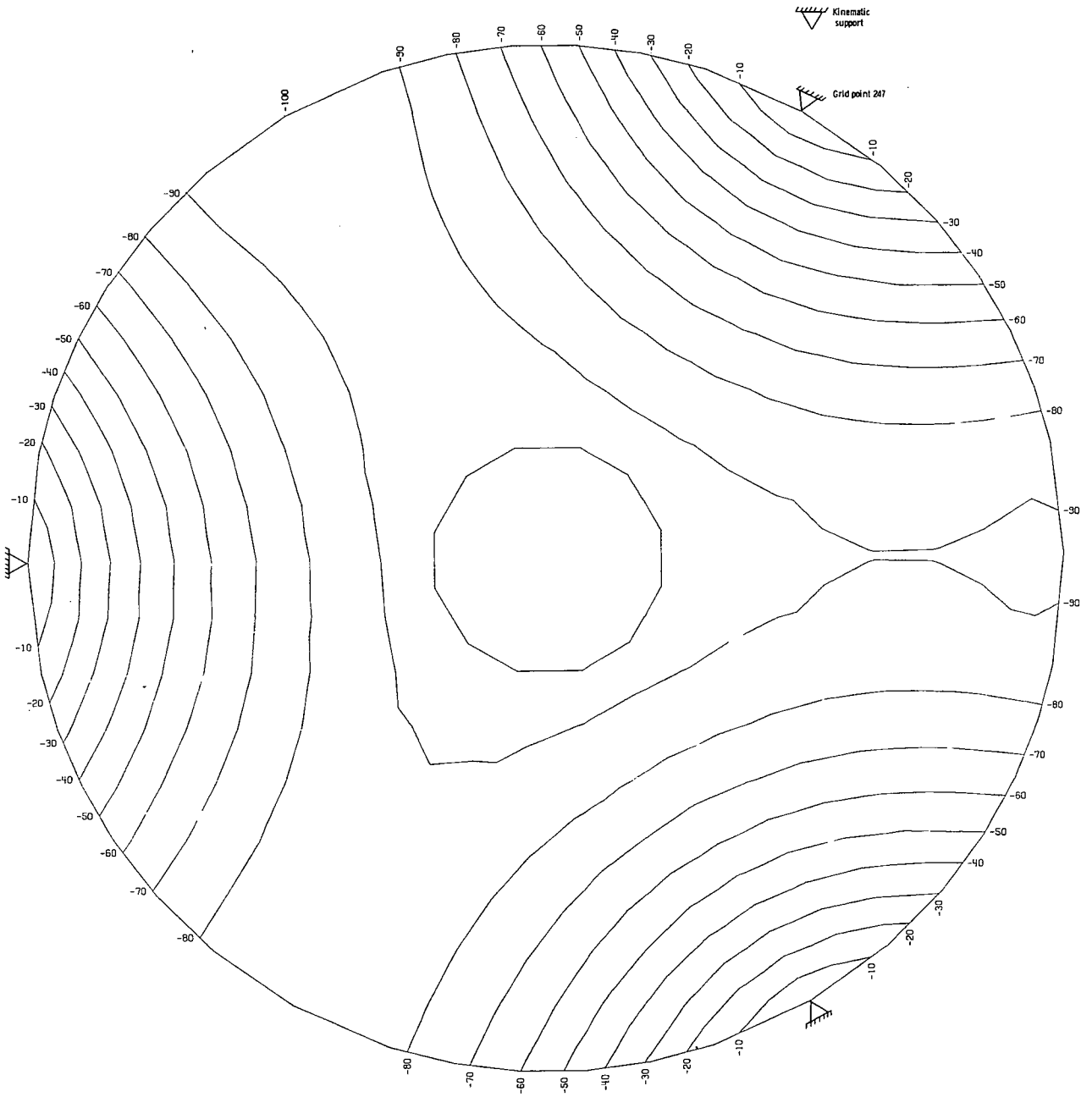

(c) Mode 3.

Figure 6.- Continued.

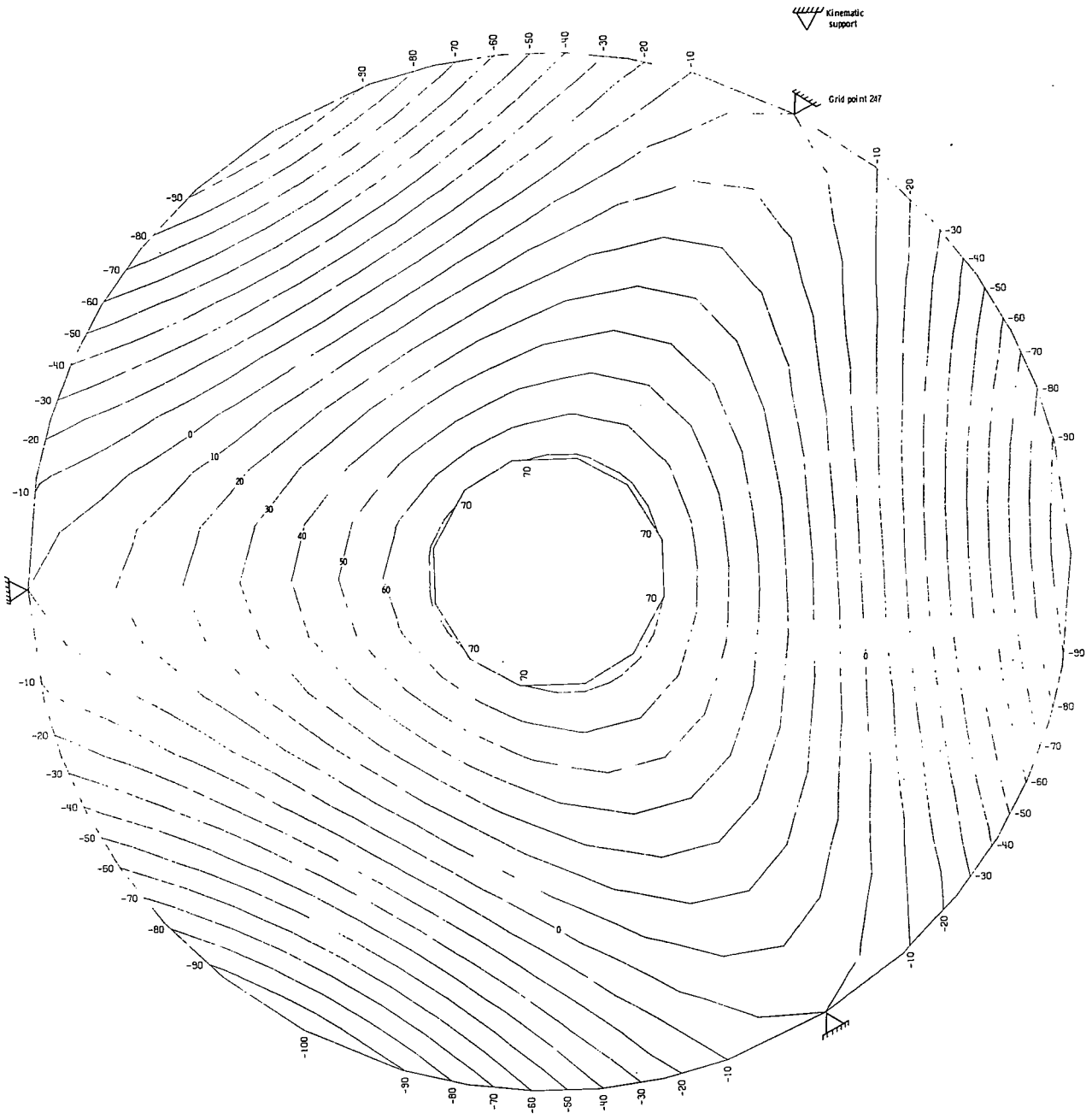

(d) Mode 4.

Figure 6.- Continued.

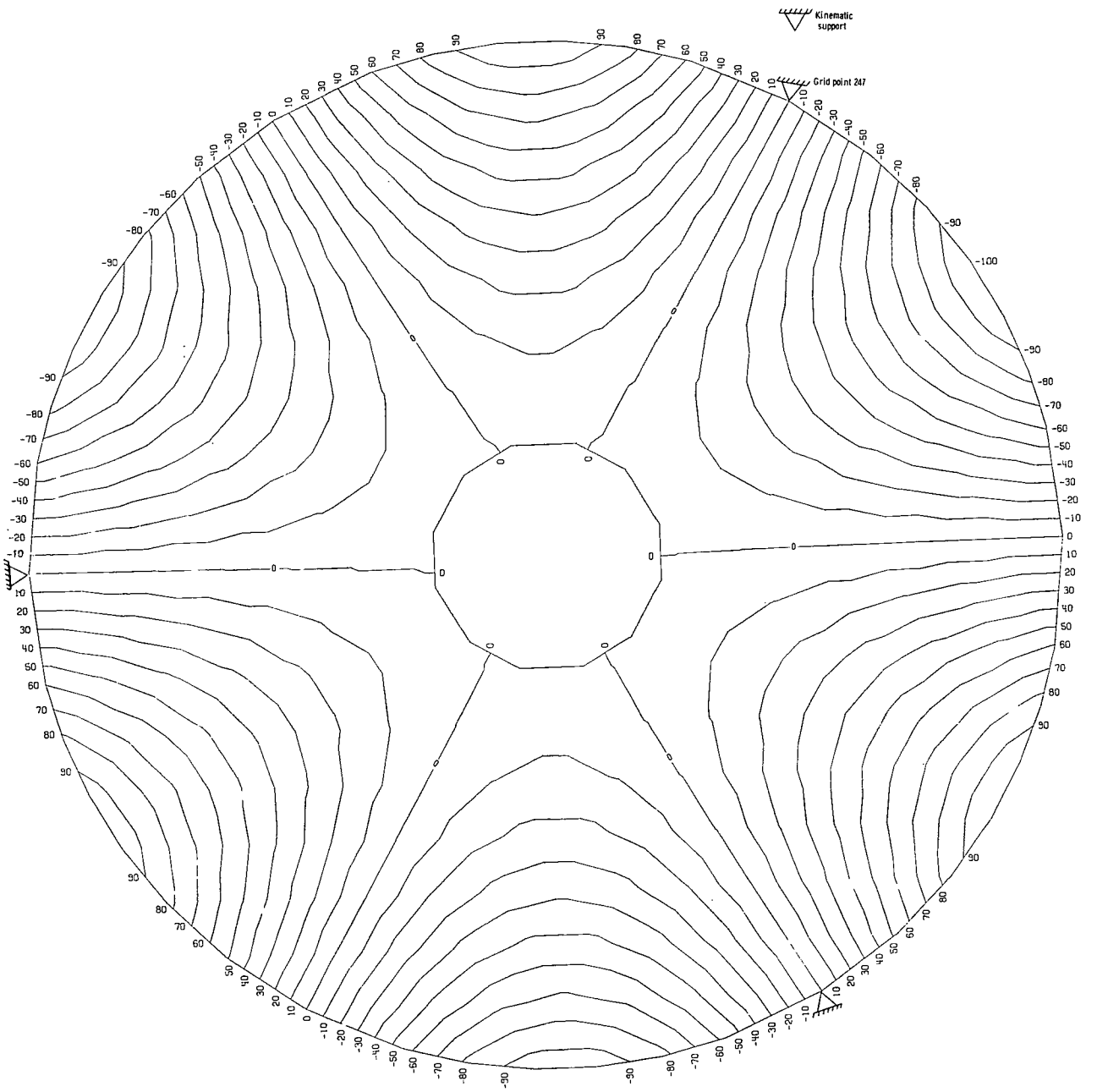

(e) Mode 5.

Figure 6.- Continued.

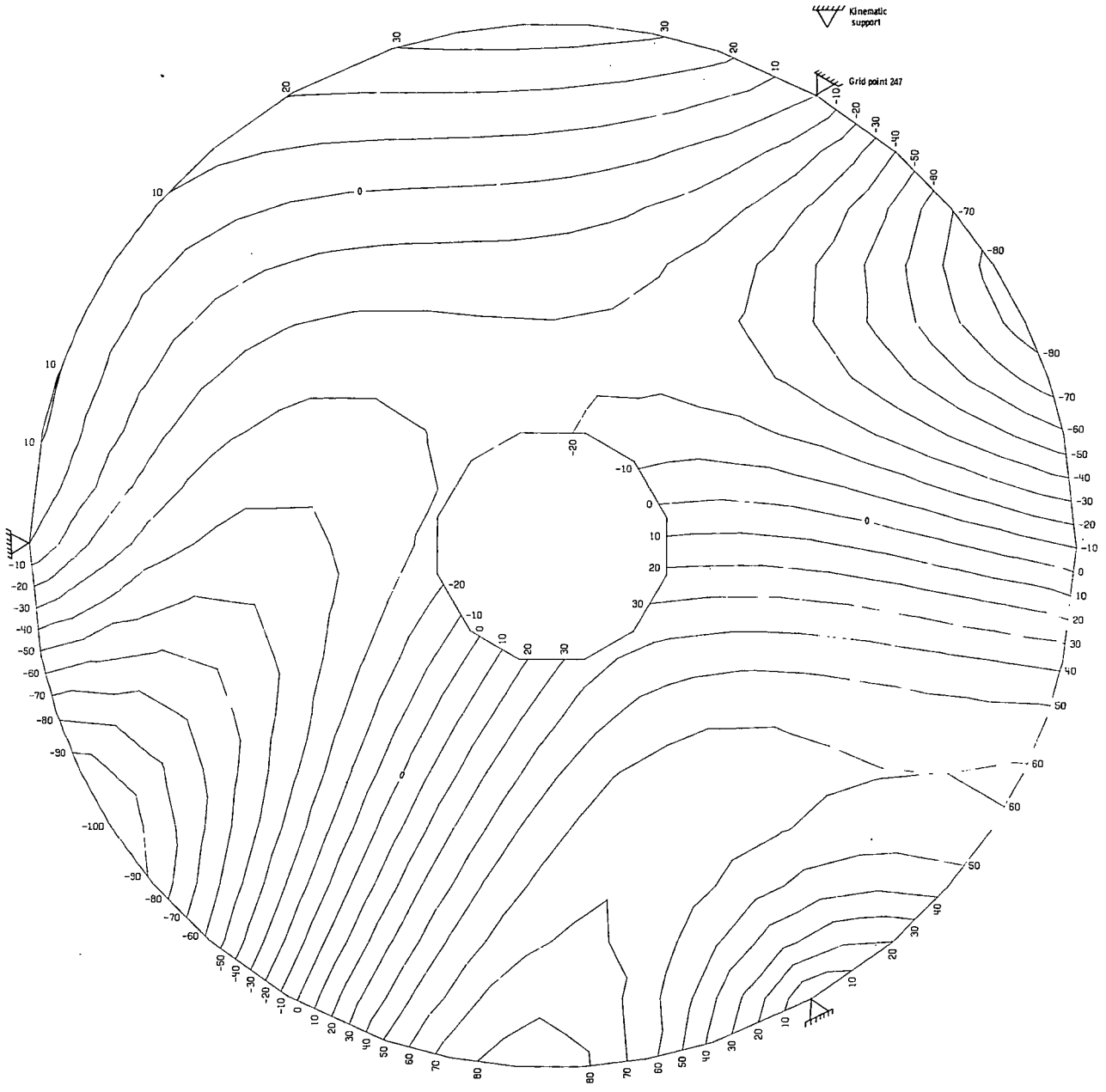

(f) Mode 6.

Figure 6.- Continued.

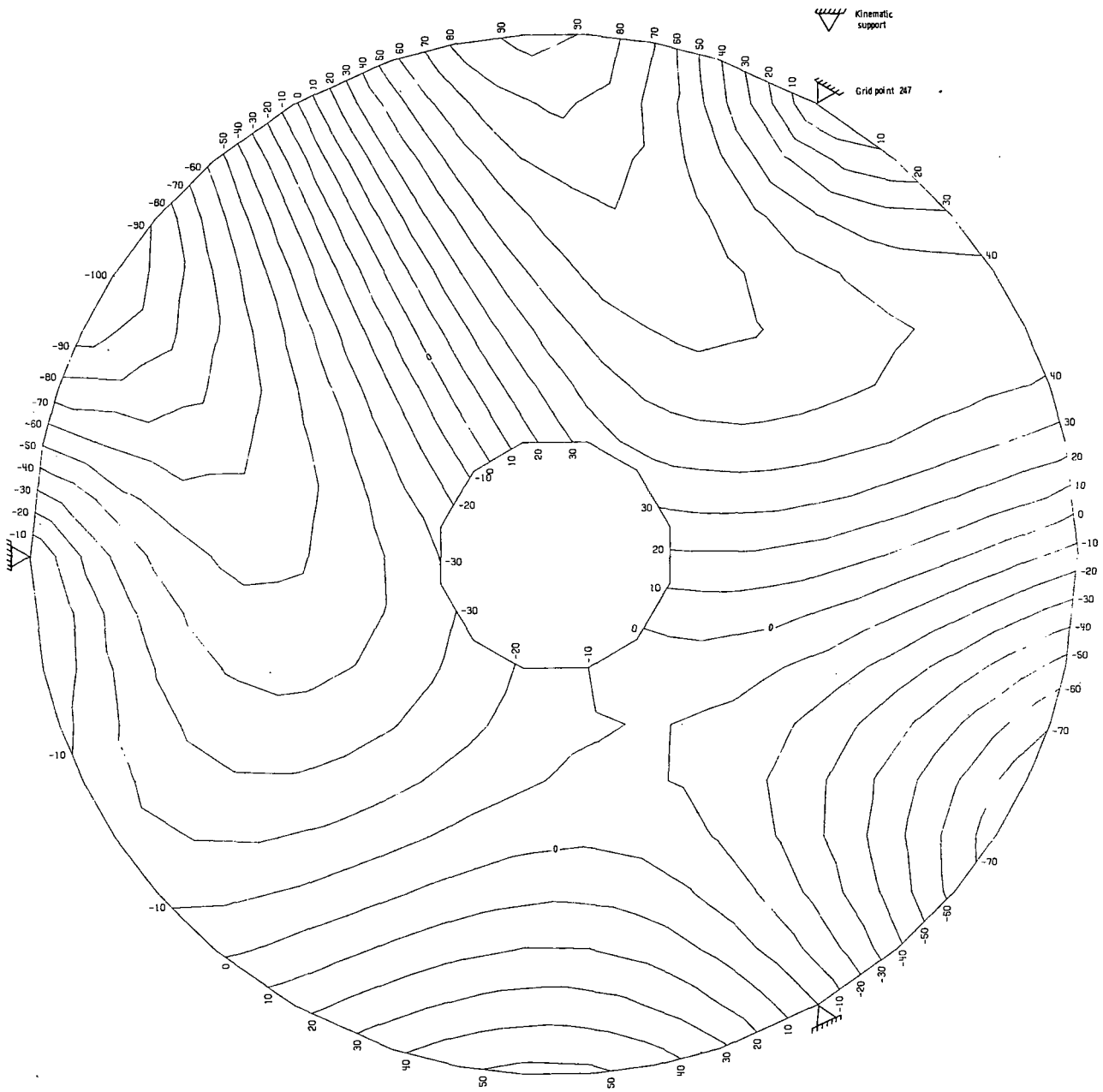

(g) Mode 7.

Figure 6.- Concluded.

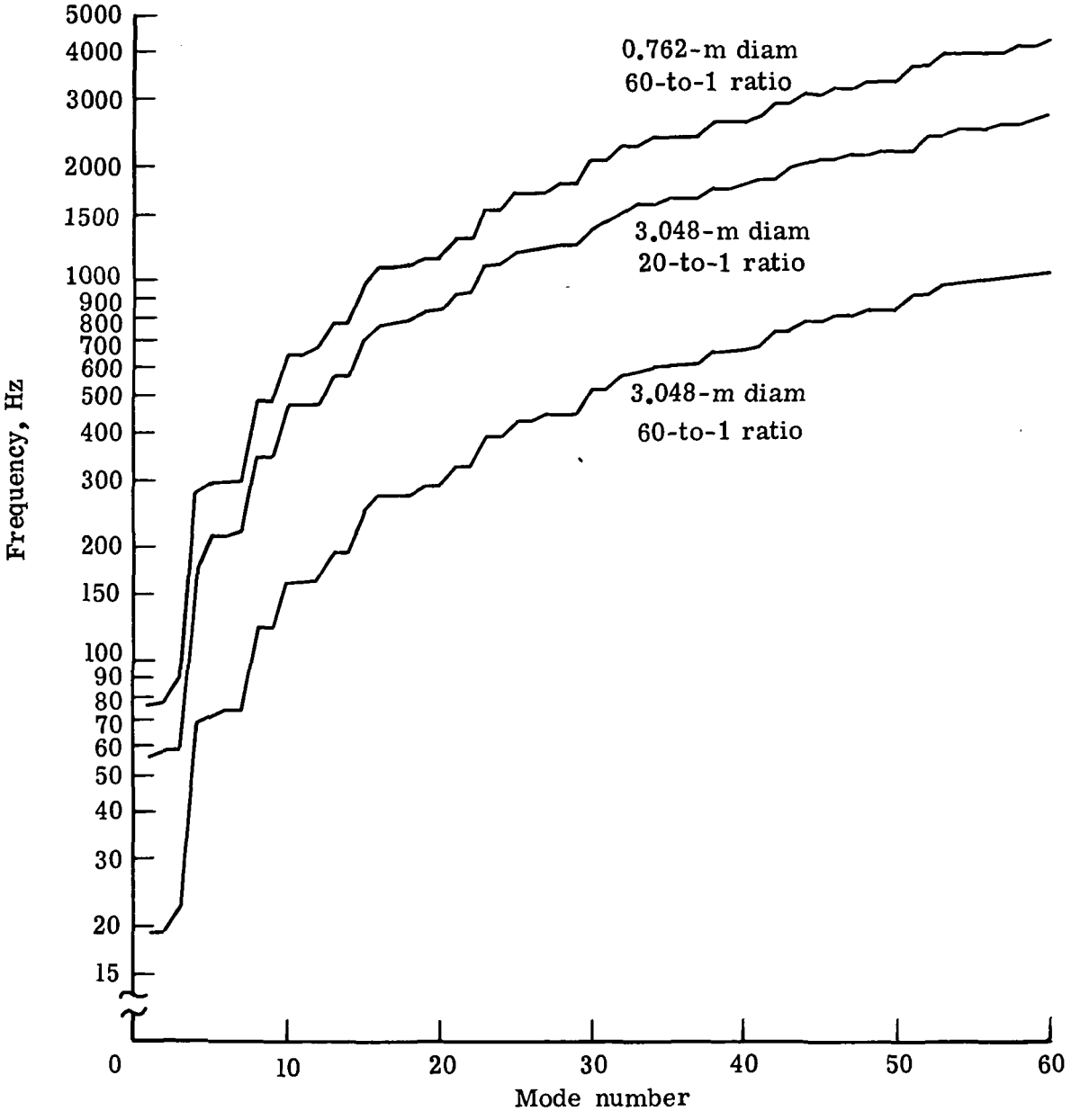

Figure 7.- Modal frequency distribution for spherical mirrors with central hole that is 22 percent of outside diameter and supports at grid points 15, 119, and 247.

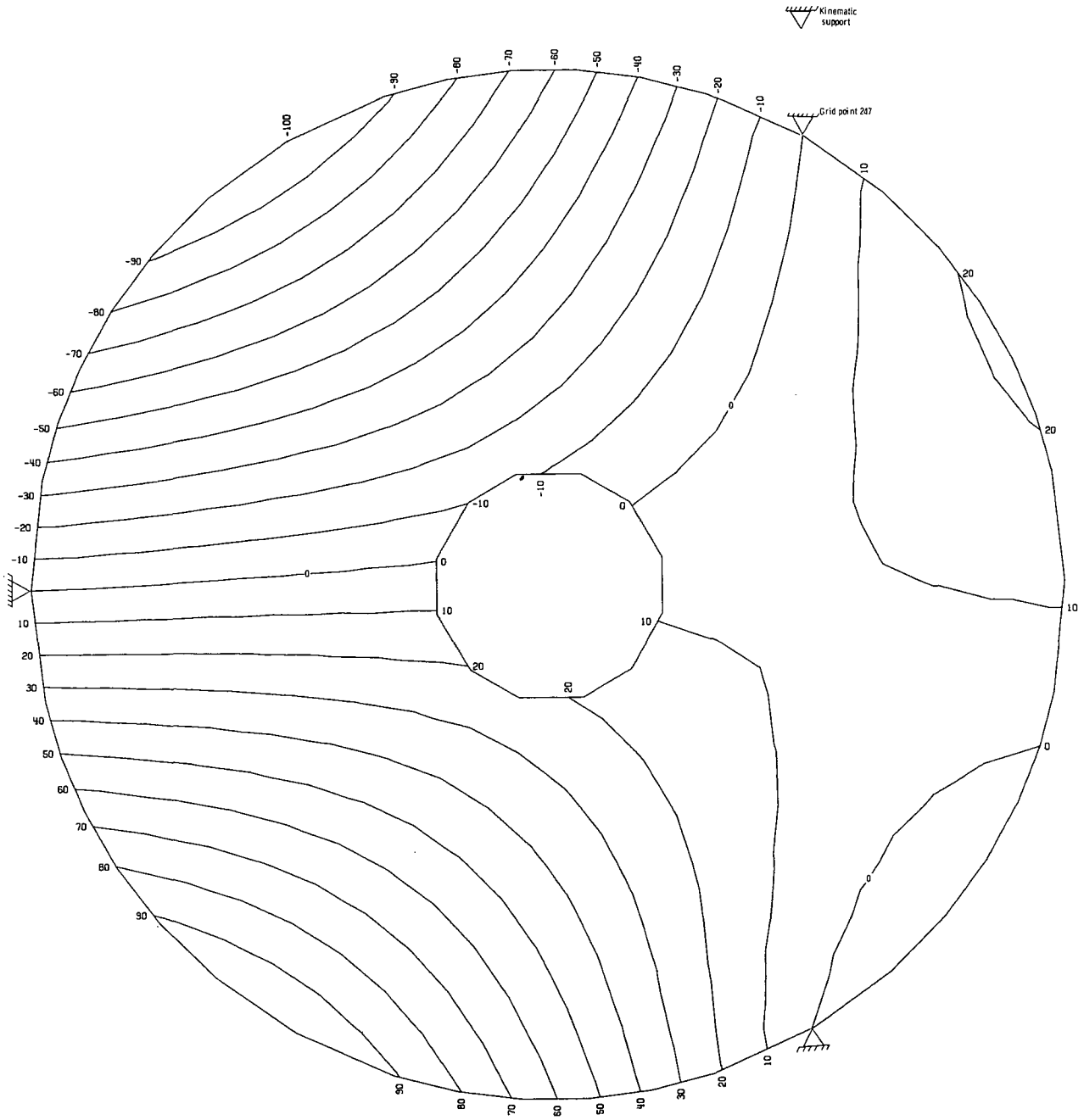

(a) Mode 1.

Figure 8.- Contour plot for 3.048-meter-diameter spherical mirror with 20-to-1 diameter-to-thickness ratio and central hole that is 22 percent of outside diameter with supports at grid points 15, 119, and 247.

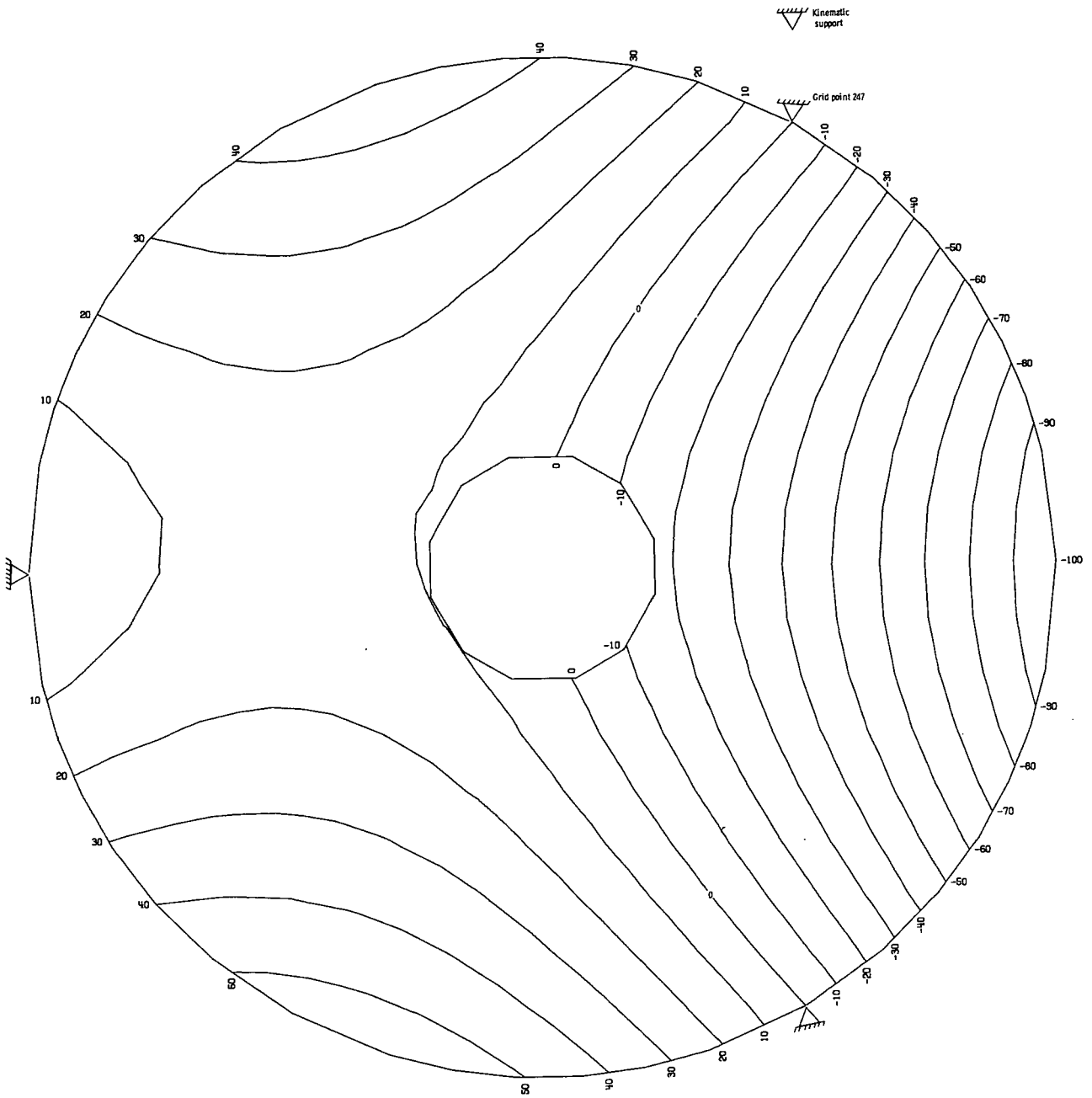

(b) Mode 2.

Figure 8.- Continued.

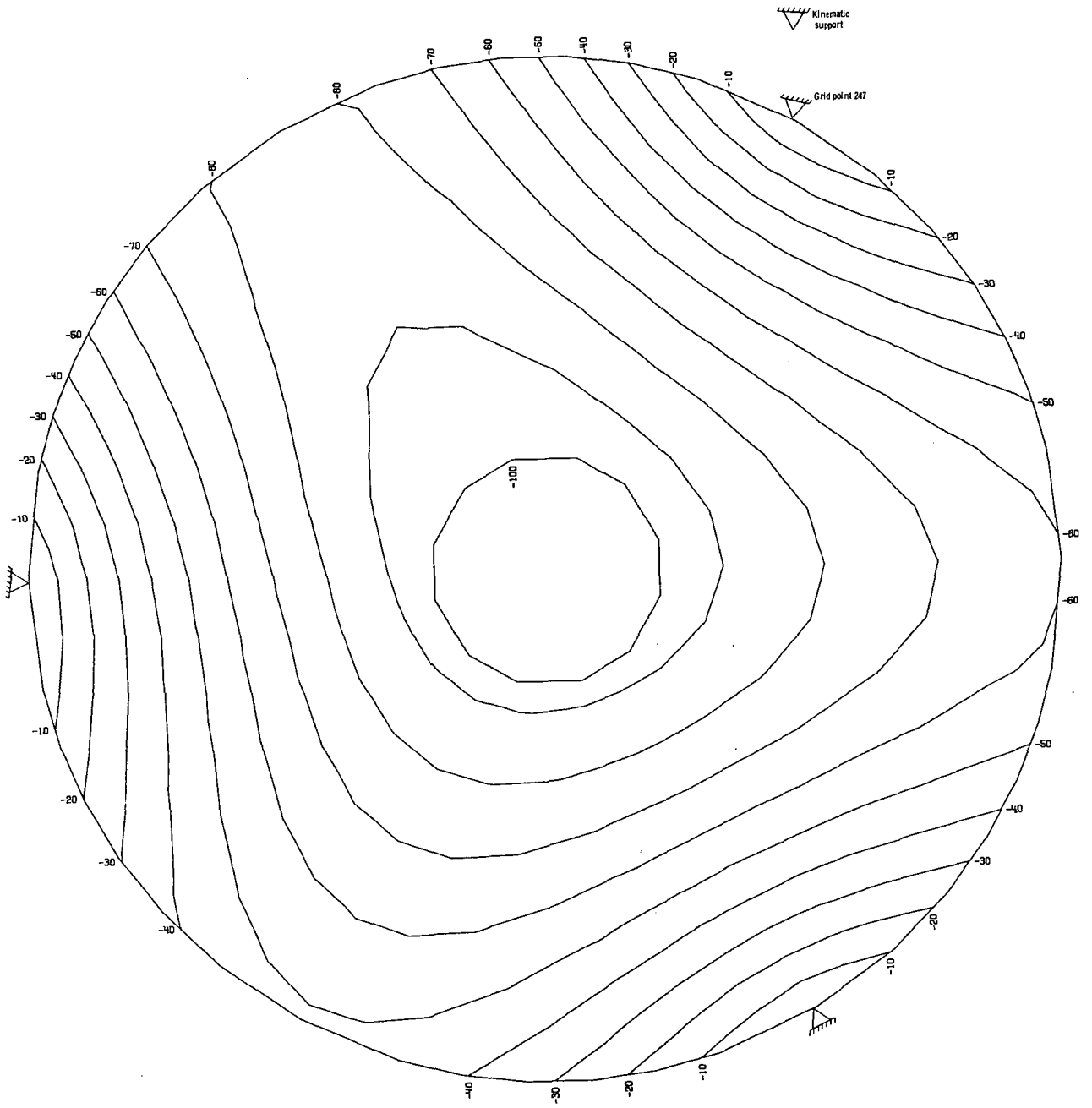

(c) Mode 3.

Figure 8.- Continued.

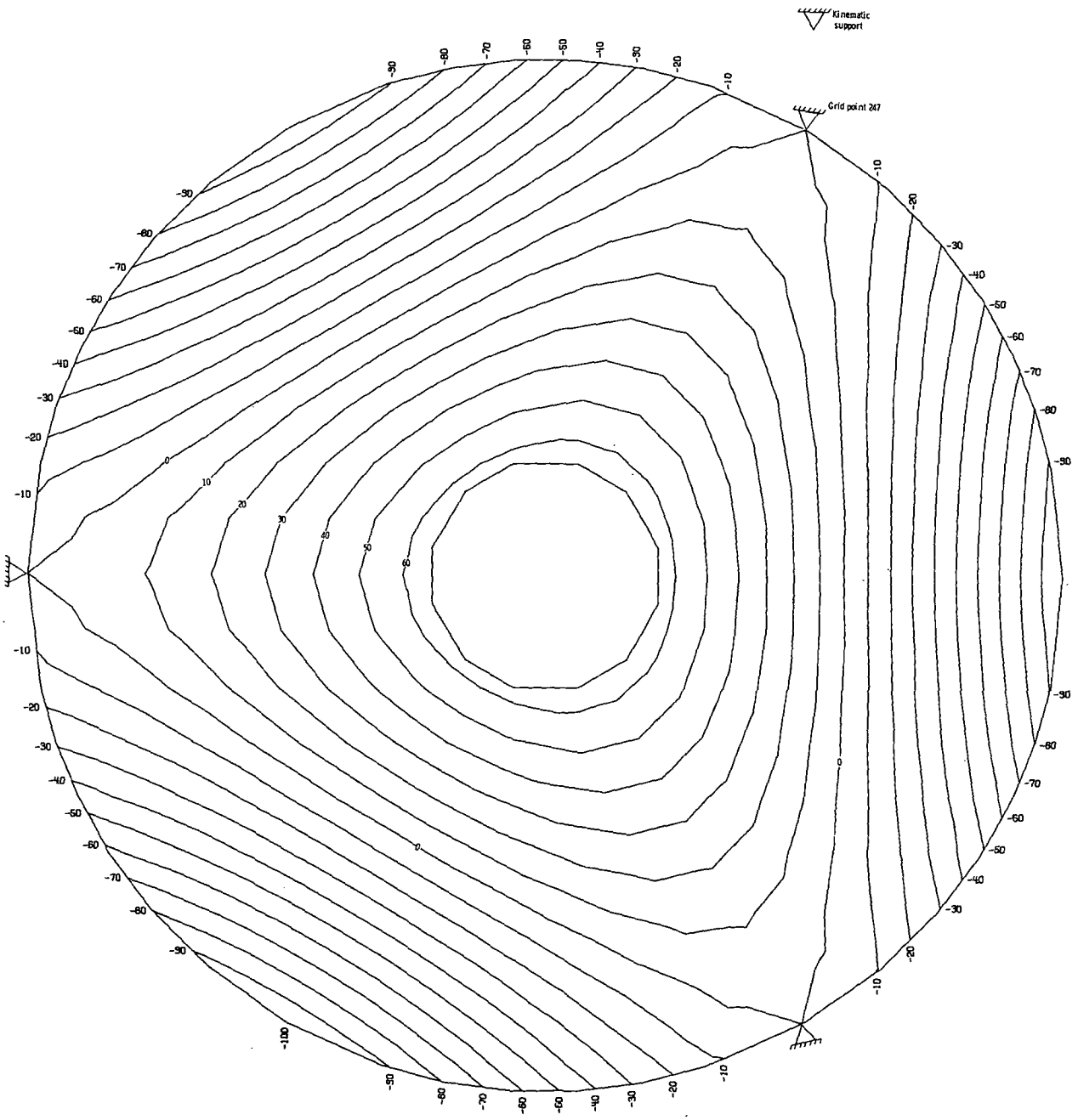

(d) Mode 4.

Figure 8.- Continued.

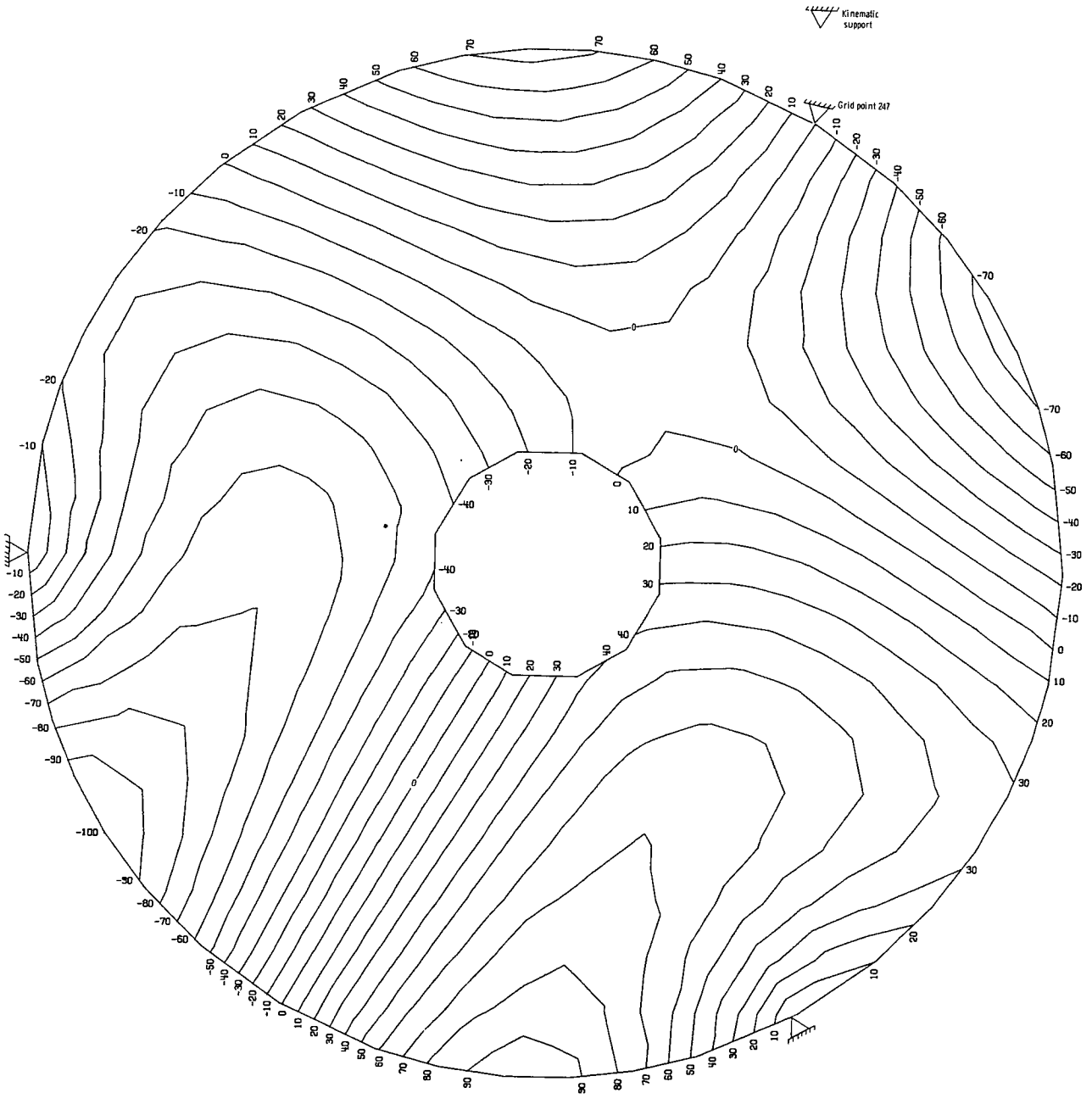

(e) Mode 5.

Figure 8.- Continued.

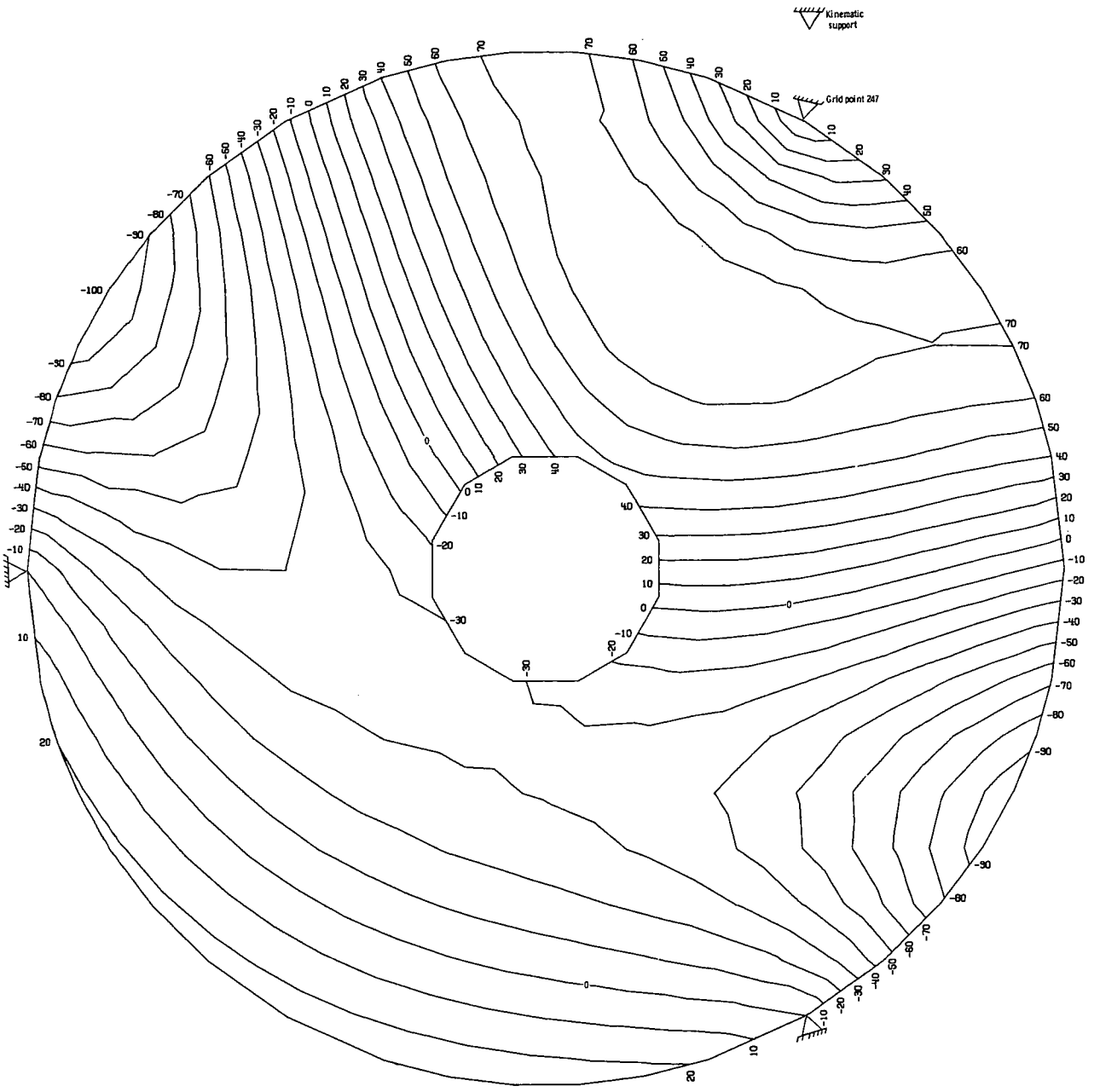

(f) Mode 6.

Figure 8.- Continued.

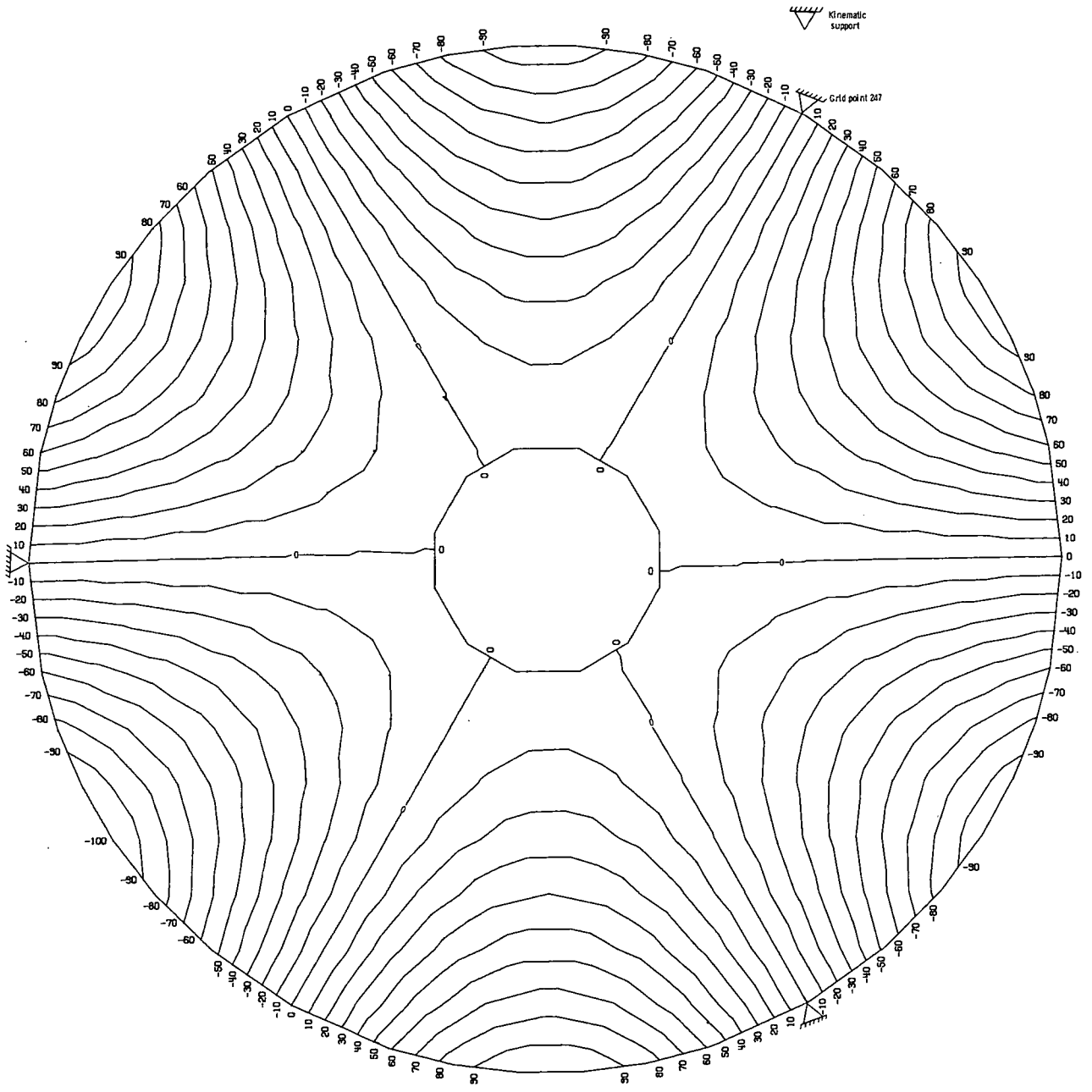

(g) Mode 7.

Figure 8.- Concluded.

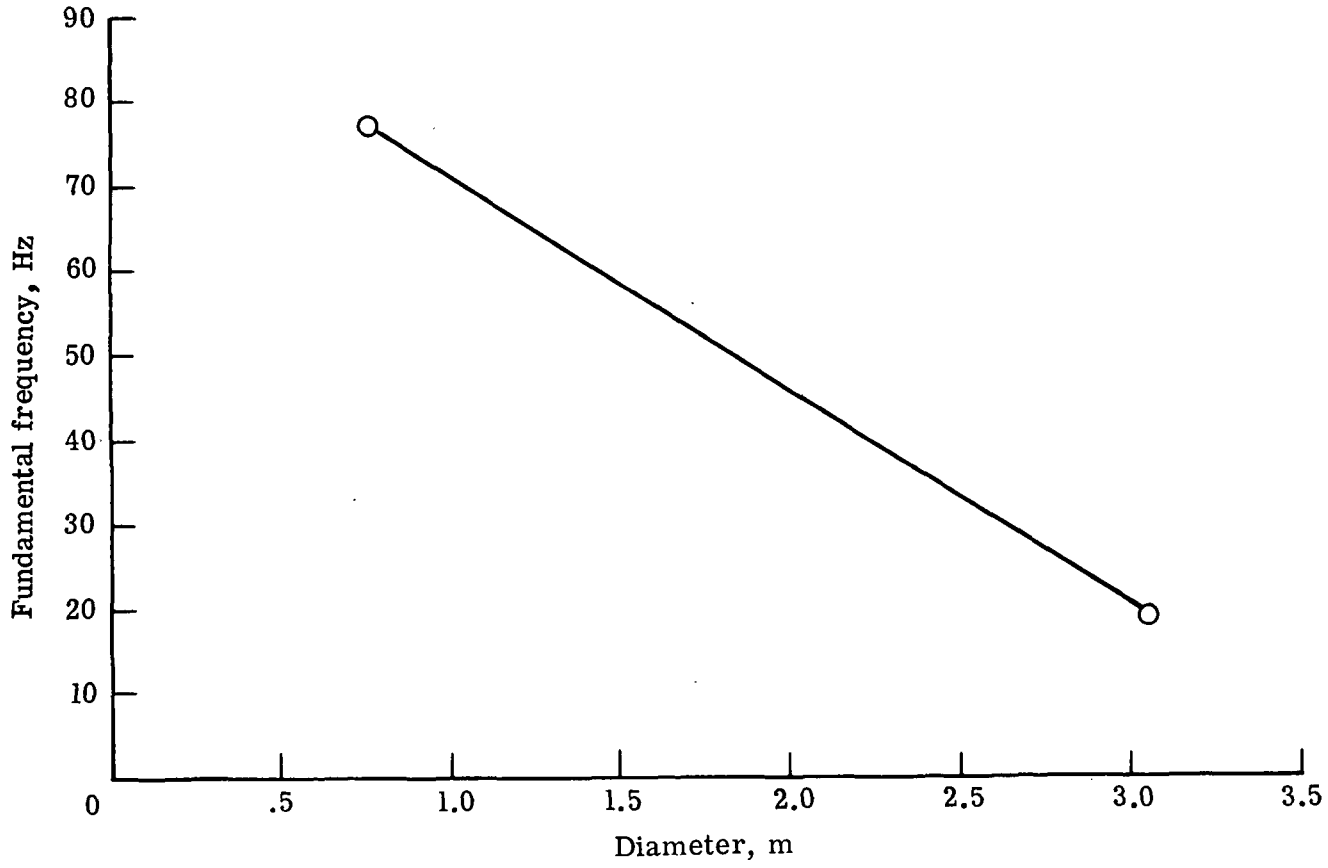

Figure 9.- Fundamental frequency as a function of mirror diameter for spherical mirror with central hole that is 22 percent of outside diameter and 60-to-1 diameter-to-thickness ratio.

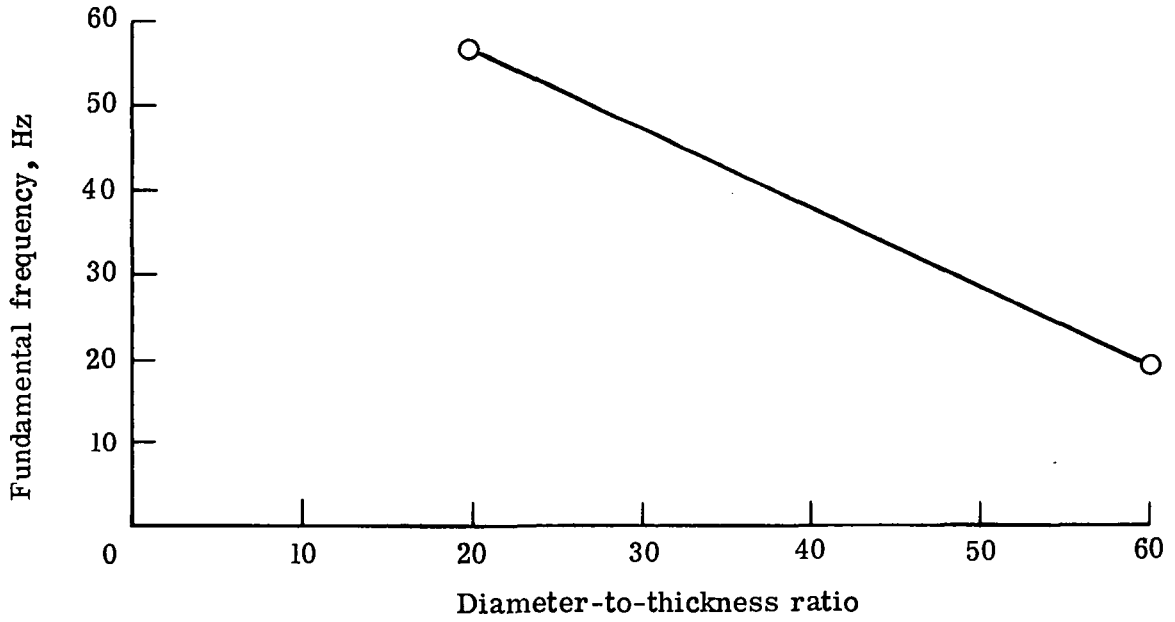

Figure 10.- Fundamental frequency as a function of mirror diameter-to-thickness ratio for 3.048-meter-diameter spherical mirror and central hole that is 22 percent of outside diameter.

NATIONAL AERONAUTICS AND SPACE ADMINISTRATION
WASHINGTON, D.C. 20546

OFFICIAL BUSINESS
PENALTY FOR PRIVATE USE $300

SPECIAL FOURTH-CLASS RATE
BOOK

POSTAGE AND FEES PAID
NATIONAL AERONAUTICS AND
SPACE ADMINISTRATION
451

U.S.MAIL

POSTMASTER: If Undeliverable (Section 158 Postal Manual) Do Not Return

"The aeronautical and space activities of the United States shall be conducted so as to contribute . . . to the expansion of human knowledge of phenomena in the atmosphere and space. The Administration shall provide for the widest practicable and appropriate dissemination of information concerning its activities and the results thereof."

—NATIONAL AERONAUTICS AND SPACE ACT OF 1958

NASA SCIENTIFIC AND TECHNICAL PUBLICATIONS

TECHNICAL REPORTS: Scientific and technical information considered important, complete, and a lasting contribution to existing knowledge.

TECHNICAL NOTES: Information less broad in scope but nevertheless of importance as a contribution to existing knowledge.

TECHNICAL MEMORANDUMS: Information receiving limited distribution because of preliminary data, security classification, or other reasons. Also includes conference proceedings with either limited or unlimited distribution.

CONTRACTOR REPORTS: Scientific and technical information generated under a NASA contract or grant and considered an important contribution to existing knowledge.

TECHNICAL TRANSLATIONS: Information published in a foreign language considered to merit NASA distribution in English.

SPECIAL PUBLICATIONS: Information derived from or of value to NASA activities. Publications include final reports of major projects, monographs, data compilations, handbooks, sourcebooks, and special bibliographies.

TECHNOLOGY UTILIZATION PUBLICATIONS: Information on technology used by NASA that may be of particular interest in commercial and other non-aerospace applications. Publications include Tech Briefs, Technology Utilization Reports and Technology Surveys.

Details on the availability of these publications may be obtained from:

SCIENTIFIC AND TECHNICAL INFORMATION OFFICE

NATIONAL AERONAUTICS AND SPACE ADMINISTRATION

Washington, D.C. 20546